Worcester Polytechnic Institute
Department of Chemistry and Biochemistry

An Investigation towards a Selective and Sustainable Separation of Rare Earth Elements through Liquid-Liquid Extraction

A Major Qualifying Project submitted for review to the faculty of
WORCESTER POLYTECHNIC INSTITUTE

In partial fulfillment of the requirements for the
Degree of Bachelor of Science

Submitted by:
Vincent N. Azzolino
Hazel A. Fargher

Project Advisor:
Dr. Marion H. Emmert, WPI Department of Chemistry and Biochemistry

2016

Table of Contents

List of Figures

List of Tables

List of Schemes

Abstract

Rare earth elements (REEs) are used in a variety of applications such as solid state lasers, magnets, MRI contrast agents, and electric motors. The U.S. currently imports all of its REEs from foreign countries, predominantly China, which puts our REE supply chain under considerable risk. One way for the U.S. to achieve REE independence is through recycling. However, there is much difficulty in separating REEs after recycling due to their similar chemical and physical properties. We investigated liquid-liquid extraction as a method of REE separation. Computational analysis was used to predict possible ligands which could selectively bind individual REEs. The synthesis and optimization of our liquid-liquid extraction method will be discussed. Furthermore, mass spectroscopy was used to study the coordination of the ligand with REEs.

Acknowledgements

We would like to thank Professor Marion H. Emmert for the mentorship she has provided both in and out of the lab through the entirety of this project. In addition Dr. Ijaz Ahmed has continued to help progress the project forward with new and innovative ideas. Both Professor Emmert and Dr. Ahmed have taught us a great deal in regards to research protocol and operating in a lab efficiently. Finally, we want to thank the rest of Emmert lab for continually giving suggestions, feedback, and support for our project since the beginning.

1.0 Introduction and Background

1.1 Rare Earth Elements

Metals have always played an important role in human development and technology. One group of metals that has recently become of global interest is the rare earth elements (REEs). These REEs are essential components in many technological applications, and as a result there is much concern over their mining, trading, and future outlook. Recycling of REEs would be an economic and environmental advantage; the problem however comes in separating the individual REEs from each other. Due to their similar physical and chemical properties, the REEs are notoriously difficult to separate.

1.2 Physical and Chemical Properties

The REEs are comprised of seventeen different elements which include the lanthanide series (elements 57 through 71) as well as scandium (21) and yttrium (39). All these elements have very similar chemical and physical properties and are generally mined as mixtures within the same ore. Scandium, yttrium, and lanthanum contain a single electron in their outermost d orbital, and the rest of the REEs are the first elements to begin to fill the f orbital. Since the f orbital is buried beneath the outermost d orbital they do not play a significant role in bonding or chemistry of the element, and so there is very little chemical distinction between the REEs.

The ionic radii trend of the lanthanide series is another unique feature of the REEs that not only affects the lanthanide series itself, but also nearby transition metals such as hafnium. In general, ionic radii decrease from left to right across a row in the periodic table. The lanthanide series, however, exhibits a much smaller decrease in ionic radius with a difference of about 0.18 Ångstroms between the largest and the smallest element. The trend is due to the poor electron shielding effect of the 4f orbitals on the 6s valence electrons which get pulled closer due to the positive force of the nucleus. As electrons are added to the f orbital the shielding remains poor, and the nuclear charge increases with each added proton, resulting in a small, but steady decrease in ionic radii.[1] Furthermore, since all the REEs are mostly found in a +3 oxidation state, their ionic radii are very close in size causing the lanthanides to exhibit similar chemical and physical properties. This phenomena was termed lanthanide contraction by Victor Goldschmidt in

1925.[2] Transition metals around the lanthanide series are influenced by this contraction as well. Element 72, hafnium, has a much smaller ionic radius than expected due to the lanthanide contraction, making its radius extremely similar to that of element 40, zirconium. Despite more than a 30 electron difference, the poor shielding and increased nuclear charge allows hafnium and zirconium to be similar both chemically and physically. This trend can be seen for the remaining transition metals past hafnium.

1.3 History of Rare Earth Elements

Since their discovery, scientists have had difficulty separating the REEs. Yttrium, the first rare earth to be discovered, was identified in 1794 by the Finnish chemist Johan Gadolin[3]. In the following years, scientists began to discover new REEs, however separation and characterization proved to be difficult. The mixture didymium, for example, was found in 1841 by Carl Mosander, who separated the mixture from lanthanum.[3] Mosander believed didymium to be an element, but it is a mixture of the REEs praseodymium and neodymium.[3] Although scientists suspected that didymium was not a pure element as early as 1853 the separation of praseodymium and neodymium was not achieved until 1882 by Professor Bohuslav Brauner.[3] The discovery of most of the REEs was through purification of rare earth mixtures.[4] The invention of the spectroscope by Kirchhoff and Bunsen in 1859 advanced the discovery of REEs, as scientists could use the unique spectroscopic bands caused by the f orbitals of the different elements as evidence of a mixture[3-4]. In 1947 Marinsky, Glendinin, and Coryell finally discovered the last REE which is the unstable and radioactive promethium[4]. While all the REEs have been found and mined, to this day they continue to prove to be difficult to separate, which effects the mining, purification, and recycling processes.

1.4 Rare Earth Uses

REEs are essential to a wide variety of applications. Common electronic devices and their components often contain several REEs. Many of the rare earths are used as a dopant in solid-state lasers since when added in trace amount which can provide the required energy state.[5] Elements such as neodymium and samarium are used to make incredibly powerful magnets due to their organization of electrons in the f orbitals.[5] REEs are used in several analytical techniques such as MRIs and NMRs. For example, gadolinium can be used as a contrast agent in MRIs as well as a

relaxation agent in NMRs. Other REEs are found in batteries, motors, cell phones, and catalytic converters.[5] Another important for REEs is as a catalyst in petroleum refining.[5] According to the USGS, the end use of REEs in 2015 is estimated to be 60% catalysts, 10% metallurgical applications and alloys, 10% ceramics and glass, 10% glass polishing, and the other 10% for other applications.[6]

1.5 Rare Earth Mining

Despite what their name suggests, rare earth elements are relatively abundant in the Earth's crust.[5] In fact, thulium and lutetium are among the least abundant REEs and are still 200 times more abundant than elemental gold.[7] However, the REEs are not concentrated in geological mineral deposits, making it difficult, inefficient, and costly to mine solely for these metals.[7] Most REEs are collected from monazite, a phosphate mineral containing a variety of rare earth oxides (REOs) and thorium, which is simply a byproduct when mining for titanium and zirconium.[7] REOs can also be mined from bastnäsite, a fluorocarbonate which contain cerium, lanthanum, and yttrium along with other REOs.[7] Although some REOs can be utilized in commercial products, most need to be reduced to the REEs before use. Whatever source they come from, REEs always come in mixtures, and so mining companies have to separate and refine them. REEs go through several separation processes, including physical sifting, magnetic separation, acidic or alkali digestion, chlorination, and organic extractions.[8] Once they have been separated, the REEs are reduced through fused salt electrolysis or metallothermic reduction, and then refined to remove impurities.[8] Not surprisingly, these processes can be energy-intensive, time-consuming and waste-intesive.

Rare earth elements are abundant around the world, but only a few countries mine them. The rare earth mine in Bayan Obo, China, is currently the top producer of REEs. In 2013, Bayan Obo mine supplied 95% of the REE market and had the world's largest supply of rare earth deposits.[7] Mountain Pass in California, which was the only US domestic REE mine up until at least 2016, reopened in 2012,[9] ten years after it closed in 2002 for environmental and economic reasons.[7] However, Molycorp, which owns the mine, filed for bankruptcy in mid-2015, making the fate of Mountain Pass mine uncertain.[10] There are other active mines located in Japan, France, and Estonia which continue to mine REOs.[11]

Due to their many uses in technological applications, countries also stockpile reserves of mined REOs. China tops for the charts with 55,000,000 tons of mined ore, and Brazil has 22,000,000 tons of mined or in reserve. In total, there are 130,000,000 tons of REO reserves available worldwide.[11] These REEs are put to use in many different areas of technology and production.

1.6 Rare Earth Independence

REEs they are an extremely valuable resource, especially in the United States. Catalytic converters, for example, made up 44% of the United States' rare earth consumption in 2006.[7] Since there are no suitable replacements for the cerium used in the converter, a halt in the REE supply chain could result in a halt in the production of catalytic converters.[7] Due to the difficulty in replacing REEs, and the risk to their supply chain, the National Research Council deemed REEs to be critical minerals.[7]

Due to their designated criticality, the United States would benefit from becoming a rare earth independent country. Over the past few decades, production and use has grown rapidly.[12] From the mid-1960s to the mid-1980s, the United States' Mountain Pass mine in California was the largest producer of REOs in the world, however in the 1990s, China quickly surpassed the United States, becoming the world's top producer of REOs.[7] In 2006, China possessed 97% of the market share of processed rare earths.[7] During the same year, the US imported 100% of its REEs from China, Japan, France and Russia, with more than 75% coming from China.[13] This put an enormous amount of dependency on imports from China which also potentially put the supply chain at risk. Making this situation more tenuous, China has steadily been decreasing the exportation of REEs. Between 2000 and 2009, the demand for REEs within China has increased by 380%, which is believed to be responsible for a 39.6% cut of Chinese REE exportation.[14] With the reopening of the Mountain Pass mine in California in 2012, the US still imported 59% of its REEs from China, France, Japan, and Estonia during 2014.[15] Although the United States had a domestic supply of 41% of REEs in 2014, the US still relied on rare earth supplies from other countries because China mines many of the heavier REEs that cannot be mined to the same extent at Mountain Pass.[12]

Furthermore, many of the heavier REEs which are not abundantly mined at Mountain Pass account for a significant percent of the current US use of REEs.[16] As a result, the United States

remains dependent on imports from foreign countries, even when Mountain Pass mine is operational.

1.7 Recycling Rare Earth Elements

One approach to achieving rare earth independence is to recycle the REEs. Recycling of REEs proves to be economically, environmentally, and socially responsible. Running and operating a mine is extremely costly, and recycling of REEs would reduce this need. The process of mining rare earths produces large amounts of waste. In 2012, the EPA conducted an in-depth report on the environmental effects of mining and recycling of REEs. The EPA discovered that the current mining techniques left a large waste footprint.[5] They also found that rare earth mining could pollute surface and groundwater, as well as sediment, soil, and air. Although it is known that long-term exposure to rare earth dust can cause pneumoconiosis in humans, a report by Hirano and Suzuki in 1996 determined that more research into better understanding the harmful effects of rare earth exposure, especially chronic exposure, was needed.[17] In contrast, after analysis of informal recycling methods of REEs, the EPA found that controlled recycling of REEs would "provide significant benefits with respect to air emissions, groundwater protection, acidification, eutrophication, and climate protection."[5]

Since REEs are found in a variety of products, they inevitably end up as waste. Considering the value of REEs, it would be important to develop techniques that allowed for recycling of these elements. Currently, there are REE containing products thrown away into landfills. Landfills are a natural resource which should not be heavily relied on for many environmental concerns, and REEs are not being used to their full potential if their end of life finds them sitting in a landfill. Recycling, on the other hand, reduces the inherent risk of importing these essential metals from other countries, and is good for the environment and society. Recent work in rare earth recycling has developed a method for a greater than 80% recovery rate of REEs from an end-of-life motor, however the REEs are recovered as a mixture.[18] The problem now comes at the separation stage. Here lies the same issue that early scientists, and modern-day mines share; REEs are extremely difficult to separate.

1.8 Rare Earth Separation Techniques

The importance of finding a method to separate the REEs seems to be widely acknowledged. Despite this, there is not much literature on REE separation, and there is still much need for further research. Nonetheless, in addition to the multi-step processes used by mines and industries today to separate the REEs, researchers have developed some other separation techniques.

1.8.1 Separation through Ion-Exchange Chromatography

One method for REE separation is through ion-exchange chromatography.[19] REEs are packed in the stationary phase of the column, and a chelating agent, such as EDTA is poured through the column.[19] While the REE cations form complexes with the chelating agents, they are not very stable complexes. The REEs that form the most stable complexes, however, will be pulled through the column faster, and will elute first. However, the eluting agent cannot always be reused, leading to a large amount of waste and expenses.[19] While this method can separate some of the REEs, but it is not yet efficient for economically stable separation.

1.8.2 Separation through Biomass Wastes Chromatography

Another method for REE separation involves using biomass in an absorption gel chromatograph. Chitosan is a polysaccharide produced by crustacean shells, which ends up as biomass waste from the marine product industry.[19] EDTA-chitosan and DTPA-chitosan can be easily synthesized using EDTA and DTPA derivatives at little cost.[19] With dilute sulfuric acid as the diluent, a column packed with EDTA-chitosan effectively separated yttrium and samarium, while a column packed with DTPA-chitosan effectively separated lanthanum, cerium, praseodymium, and neodymium.[19] Despite having good separations, there are some drawbacks to using this method. Most importantly, this method cannot separate the heavier REEs. The heaviest element separated, samarium (molar mass = 150.36 g/mol), can only be separated from the lightest element, yttrium (molar mass = 88.91 g/mol). In addition, column chromatography produces a lot of waste, and so is not the most efficient method for separation.

1.8.3 Separation through Solvent Extraction

A promising method of REE separation is through solvent extraction. Solvent extraction uses the phase separation of aqueous and organic solvents to separate the REEs. In their ionic form, the REEs dissolve in an aqueous solution. An organic extractant that dissolves in an organic solvent could bind with an REE ion, and pull it into the organic phase, as shown in Figure 1. If an extractant were selective for one REE over all the others, that REE would be pulled into the organic phase and could be isolated from the mixture of REEs by simply separating the organic phase from the aqueous phase. Once the phases have been separated, the rare earth must be stripped from the organic extractant in order for it to be recovered. One draw-back is that because an extractant is selective for one REE, one extractant must be synthesized for each REE. This method has been researched with phosphonic and phosphinic acid extractants.[20]

1.9 Lanthanide – Actinide Separation

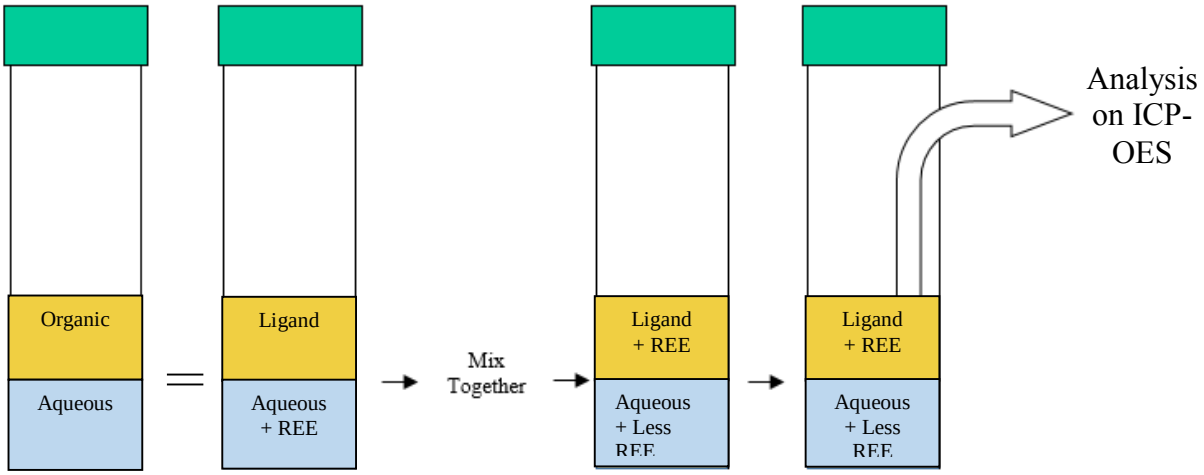

Figure 1: Liquid - Liquid Extraction

Despite a lack of research into REE separation, there has been significant research into the separation of actinides from lanthanides. Waste from nuclear power plants is often a mixture of lanthanides and the highly radioactive actinides. Separating actinides from lanthanides helps to reduce the amount of radioactive waste that must be properly disposed of and treated. Research went into liquid-liquid extractions, and in 1999, Kolarik et al. showed that 2,6-bis(5,6-dialkyl-1,2,4-triazin-3-yl)pyridine, or BTP (Scheme 1), was able to extract Am(III) over Eu(III) in nitric

acid.[21] This led to further research into BTP and BTP derivatives for lanthanide and actinide separations such as $CyMe_4$-BTBP (Scheme 2) which is highly selective for Am(III) over Eu(III) and can withstand harsher conditions than BTP.[22] Further work was done by Geist et al. in 2006 showed that $CyMe_4$-BTBP were one to two orders of magnitude more selective for actinides over lanthanides when used in liquid-liquid extraction.[22] Due to the success of liquid-liquid extraction in separating the lanthanides and actinides, we are investigating the same method for the separation between lanthanides and lanthanides.

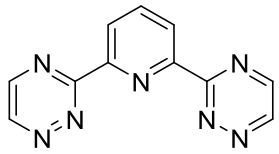

Scheme 1: BTP molecular structure.

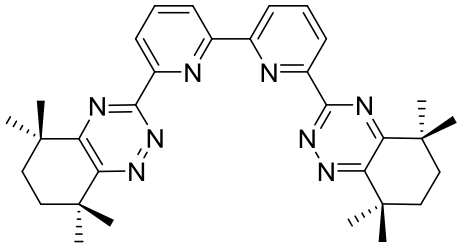

Scheme 2: $CyMe_4$-BTBP molecular structure.

1.10 Project Goals

We are investigating the separation of REEs through solvent extraction. The goal of our project is to design organic extractants that can selectively extract a REE out of an aqueous phase and into an organic phase. Although changes in ionic radii of the rare earths are small, with only a 0.18 Å difference between lanthanum, the largest of the rare earths, and lutetium, the smallest, our hypothesis is that small changes in the organic extractant can greatly change selectivity by providing a unique "fit" for a given REE. Furthermore, this project strives to understand the basic coordination chemistry that lanthanide elements exhibit with these new ligands.

1.11 Knowledge at Project Start

Work by Geist et al. in 2006 showed that $CyMe_4$-BTBP was more selective for Eu(III) over the other REEs.[22] Additionally, selectivity for an REE(III) ion increased as the ionic radii became closer in size to the ionic radii of Eu(III).[22] This led to our hypothesis that BTP is most selective for Eu. More generally we hypothesize that BTP and BTP derivatives are selective for an REE ion depending on the ligand's binding pocket size, and the size of the REE ionic radii. This hypothesis

was further tested by Kathleen D. Field with computational analysis through the Gaussian 09, B3LYP, 6-31G(d) computer program. The program changed the orientation of BTP and some derivatives until the geometry produced the lowest strain energy. Once an optimized geometry was found, the vibrational frequencies were optimized by finding the minimum value of the second derivative of this geometry.[23] The distance between nitrogen groups and the dihedral angle of the optimized ligand were calculated, and a three dimensional model of the molecule could be viewed and analyzed. It was proposed that different sizes and bite angles of the bonding pocket of the extractant would selectively chelate different REEs due to their slight differences in ionic radii. This angle gives an idea of what orientation the ligand will chelate the metal as well as the effect on chelating ability when the angle is different. Optimizing this angle can enhance the selectivity of an extractant. It is within these variables that small changes must be made in order to accommodate the miniscule changes in ionic radii of the REEs. In addition to optimizing these ligands without metals, this program can optimize geometry and frequency while coordinated to any of these rare earth elements and further analysis can be run. Computational work done by Kathleen Field agreed with the hypothesis, showing that BTP and Me_4-BTP would preferentially bind to Eu over the other rare earth elements, because the size of its ionic radii was the best fit in the binding site.

1.12 Approaches Taken Within the Scope of this MQP

We are investigating the separation of REEs through solvent extraction. We have approached this problem with a four-step method. Figure 1, see page 17 above, outlines this approach. The process begins with computational analysis of a potential organic extractant with Gaussian, as explained in section 1.11. BTP and its derivatives were chosen as a starting point due to its unusual selectivity for Eu(III), as mentioned in section 1.11. Computational work for this project was done by Kathleen Field. And revealed which ligands were theoretically selective for an REE. The next step was to synthesize the extractant so that it can be characterized and tested in the lab. The ligand-metal bonds were then characterized in order to determine how the extractant complexes with the metal in order to pull it from the aqueous phase. Finally, the synthesized extractant is used in an extraction to investigate how well the molecule can separate the REEs. All this information is then used to update the computer model and to computationally design a better extractant, or find one that is selective for a different REE.

2.0 Results and Discussion

The purpose of this investigation was to develop a computational model of potential ligands for the extraction of REEs, synthesize those ligands, characterize them, perform extractions on REEs with them, and then use the new information to further improve the computational model. Throughout this investigation, we investigated two organic ligands: BTP and Me_4-BTP.

2.1 Synthesis

2.1.1 Me_4-BTP

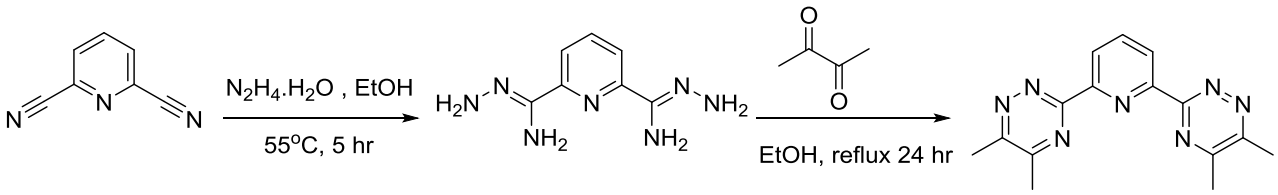

Scheme 3: Synthesis of Me4-BTP from dicyanopyridine.

Me_4-BTP was synthesized from a dicyanopyridine through two steps (Scheme 3). Dicyanopyrdine was reacted with hydrazine monohydrate in ethanol at 55°C for 5 hours to form the dicarbamidrazone intermediate with a 93% yield.[24] The intermediate was mixed with 2,3-butadione and refluxed in ethanol for 24 hours to give a 70% yield of the product.[24]

2.1.2 BTP Literature Synthesis

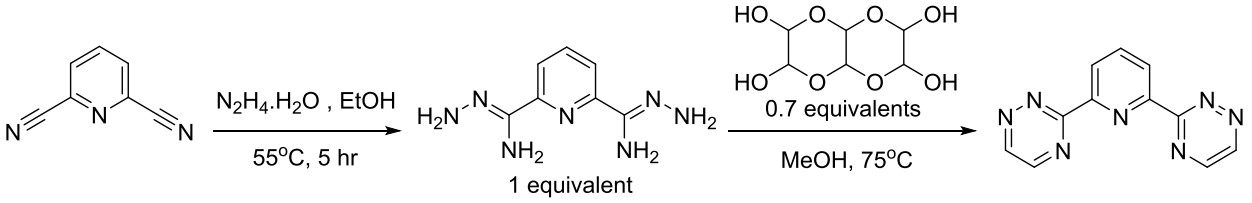

Scheme 4: Literature synthesis of BTP.

At the beginning of this project, BTP was synthesized from dicyanopyridine in two steps (Scheme 4). Dicyanopyrdine was reacted with hydrazine monohydrate in ethanol at 55°C for 5 hours to form the dicarbamidrazone intermediate with a 93% yield.[24] The intermediate was mixed

with glyoxal trimer dihydrate in methanol at room temperature for 3 hours, and then heated to 75°C for 2 hours.[21] This literature method always resulted in an impure product with lower yields than expected (82% yield).

2.1.3 Purifying BTP

When the synthesis of BTP resulted in an impure product, purification of the BTP was difficult. Because of its low solubility in all of the organic solvents tested, recrystallization through layering of BTP was not successful. Instead, a silica pad could be used to clean the BTP which came out in the third fraction. Although this method produced clean BTP, very little product was recovered, and a wasteful amount of DCM was used. Because of this, a silica pad could not be used for purification of BTP on a large scale.

2.1.4 Optimizing BTP Synthesis

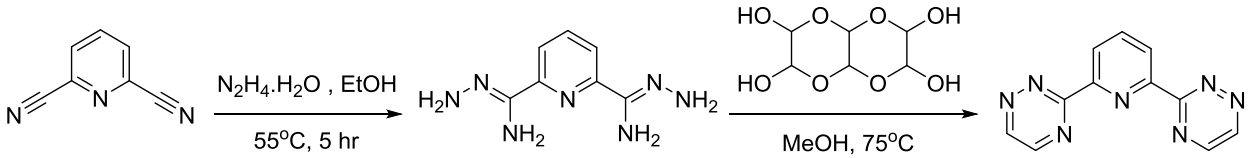

Scheme 5: Optimizing BTP synthesis.

Because the literature method of synthesizing BTP often resulted in poor yields ranging from 21% to 50% and an impure product, the conditions for the BTP synthesis were optimized and improved in order to get the highest yield of clean BTP (Scheme 5). Samples differed by number of equivalents of glyoxal trimer, amount of time stirred at room temperature, and amount of time heated. Samples were analyzed through GC using phenyl bromide as the internal standard. Yields were determined by using Equation 1, the calibration equation for the GC.

$$mmol\ BTP = 1.8272 \times \frac{Area_{sample}}{Area_{PhBr}} \times 0.095\ mmol\ PhBr$$

Equation 1

Under best reaction conditions, 1 equivalent of glyoxal trimer dihydrate and 1 equivalent of dicarbamidrazone intermediate were stirred in methanol at room temperature for 2 hours and

then heated for 3 hours at 75°C. Figure 2 shows the GC spectra of this condition, with phenyl bromide at 3.72 minutes with a 2.05% area and the BTP peak at 10.84 minutes with a 0.58% area. These percent areas gave the 95% yield. The literature condition was also run as a control, in which 0.7 equivalent of glyoxal trimer dihdyrate and the dicarbamidrazone intermediate were mixed in methanol at room temperature for 3 hours, and then heated at 75°C for 2 hours. A similar GC spectra for the literature method gave a 1.69% area of phenyl bromide and a 0.00046% area of BTP. This gave a 0.09% yield.

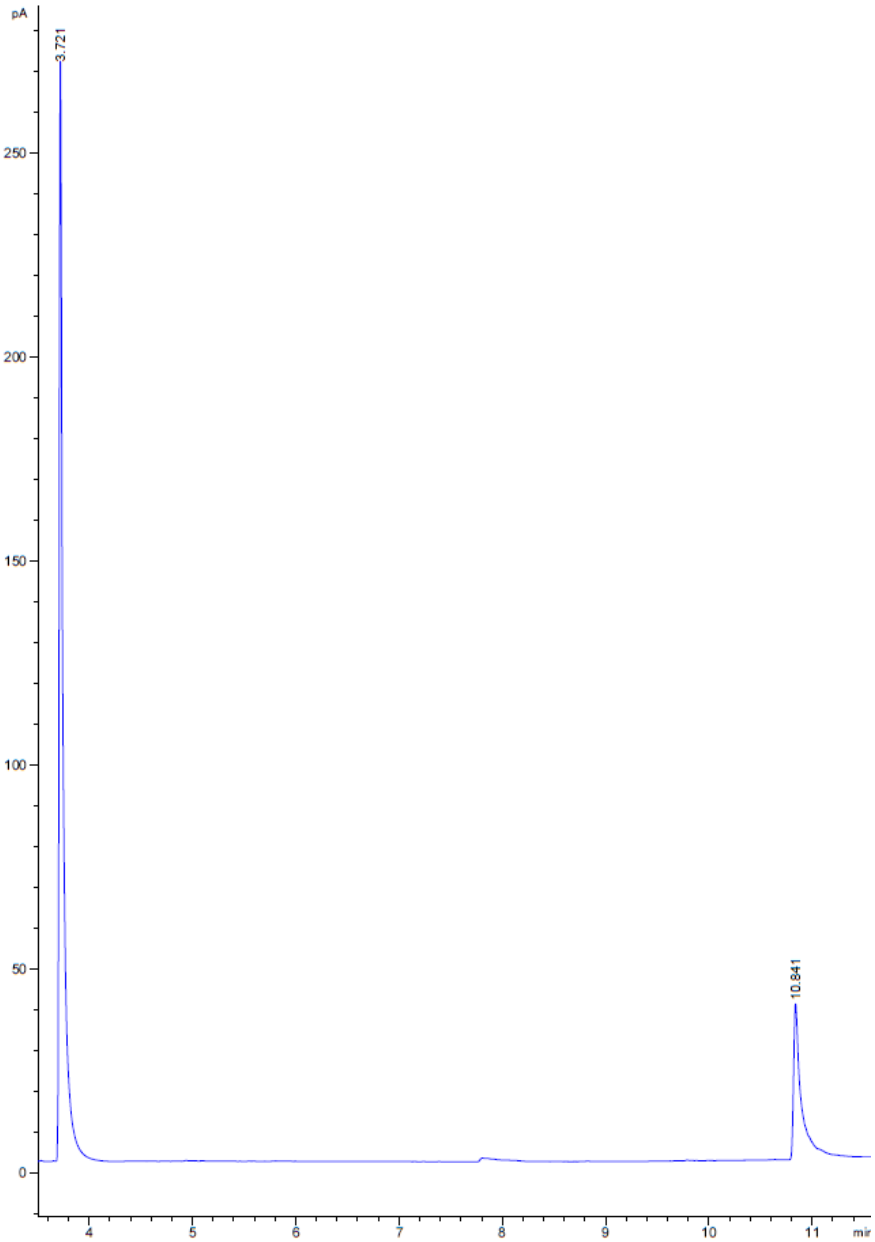

Figure 2: PhBr and BTP peaks on the GC spectra of sample 1HAF-94-H.

The solvent also had a large impact on the purity and amount of product produced. The optimized reaction was then run in 99.8% pure MeOH which had been dried with activated molecular sieves specifically designed to absorb water. The purity of the reaction was greatly improved. We conclude that water must interfere in the reaction and produce unwanted side products.

Through this work, we have optimized the literature BTP synthesis. The optimized BTP synthesis requires 1 equivalent of intermediate, 1 equivalent of glyoxal trimer dihydrate in 99.98% pure MeOH dried over molecular sieves. This solution is stirred in a flame-dried round bottom flask at room temperature for two hours under nitrogen gas. The reaction is then heated to 75°C for three hours. Once the reaction is complete, it is cooled to room temperature, stored in the freezer overnight, and then the product is vacuum filtrated and dried. This new reaction has a 95% yield and produces clean BTP.

2.2 Solubility Studies

2.2.1 BTP

The original ligand designed by Kolarik to chelate REEs was BTP.[19] However, because chloroform was not polar enough, BTP was only slightly soluble in chloroform. As a result, a solution of BTP in $CHCl_3$ was not uniform which meant that the extractions run under this solvent system were inconsistent, causing large standard deviations. To optimize the solubility of BTP, several different solvent systems were tested. BTP was never completely soluble in a solvent solution, but the compound made the most uniform solution in a solvent system of chloroform and methanol in a 9 to 1 ratio. This first solvent study provided useful information in optimizing a solvent system for BTP. In the first study, when water was used as a solvent the solutions precipitated BTP and caused a phase separation. The chloroform and water were not miscible and caused separation more easily. With the addition of methanol, the organic and aqueous layers became more miscible, and BTP precipitated at the bottom of the vial. However, when the solvent system only included the organic solvents chloroform and methanol, BTP formed a uniform solution without phase separation or precipitation of BTP. The results from this trial are shown in Figure 3.

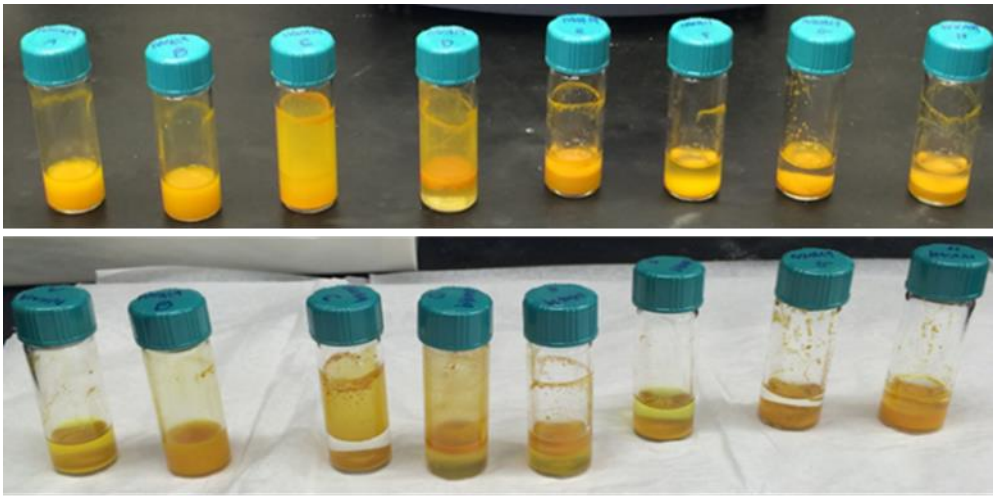

Figure 3: Solubility Study - Left to Right: 1:1 Chloroform: Methanol, 9:1 Chloroform: Methanol, 1:1 Chloroform: Water, 9:1 Chloroform: Water,2:1:1 Chloroform: Methanol: Water, 1:2:1 Chloroform: Methanol: Water, 1:1:2 Chloroform: Methanol: Water, 1:1:1 Chloroform: Methanol: Water. Top: 10 minutes Bottom 72 Hours.

In order to avoid the mixing between aqueous and organic phases caused by methanol, a new solvent system was tested containing different ratios of chloroform and octanol. The methanol was replaced by octan-1-ol. BTP made a uniform solution in chloroform and octanol in a 19 to 1 ratio. Mixtures with varying ratios of chloroform to octanol were all very similar in appearance after several hours. Only after a few days did a difference become apparent between the different samples. The chloroform and octanol with a 19 to 1 ratio best maintained the uniform solution. Unfortunately none of these solutions were capable of producing a solution which completely dissolved BTP. However, a uniform solution provided a way to create reproducible extractions with lower standard deviations. As a result of this trial, extractions were run with a 0.05 M solution of BTP in 9.5 ml of $CHCl_3$ and 0.5 ml of octanol.

2.2.2 Me_4-BTP

Figure 4 shows the results of the solubility studies of Me_4-BTP. The four methyl groups on the Me_4-BTP made the molecule greasier, and allowed it to more easily dissolve into organic solvents. As a result, the ligand was completely soluble in the nonpolar solvents $CHCl_3$, DCE, and DCM. Me_4-BTP becomes less soluble in ethyl acetate, and insoluble in water, PhCl, PhBr, and $PhCF_3$. The ligand also became a uniform suspension in octan-1-ol. Due to the high solubility of Me_4-BTP in $CHCl_3$, we first investigated REE extraction with this ligand.

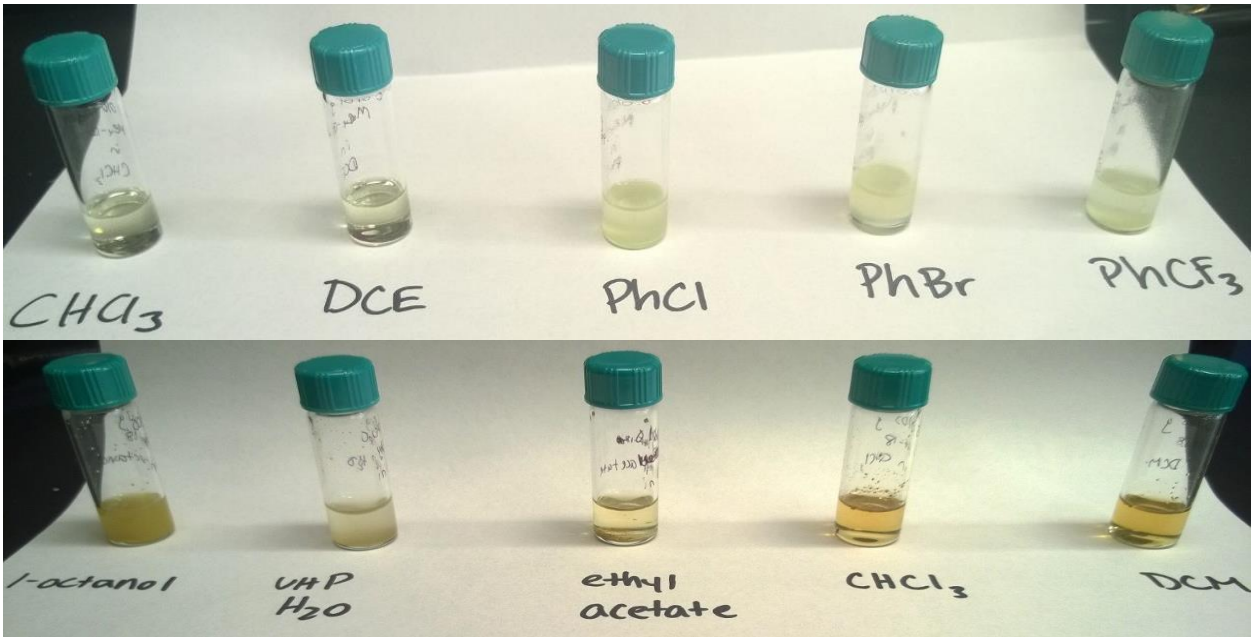

Figure 4: Me_4-BTP Solubility Study: solvent mixtures

2.3 Work on Me_4-BTP

2.3.1 Extractions with Me_4-BTP

Computational models predicted that Me_4-BTP would be selective for Eu over the other REEs. To test this, an extraction of 0.002 M Eu in 0.001 M HCl by 0.05 M Me_4-BTP in $CHCl_3$ (Scheme 6 below) was run. Experiments showed very little extraction of the Eu into the organic phase, with extractions around 5%. This extraction was improved to about 65% by adding 5 drops of aqua regia to the ICP-OES sample preparation (Scheme 6). However, this percent extraction could not be replicated in later experiments using 1 ml aqua regia during the ICP-OES sample preparation (Scheme 6). Finally, through all the experiments shown in Scheme 3, the relative standard deviation over three trials remained above 10%. The experiments showed that Me_4-BTP did not consistently extract Eu very well.

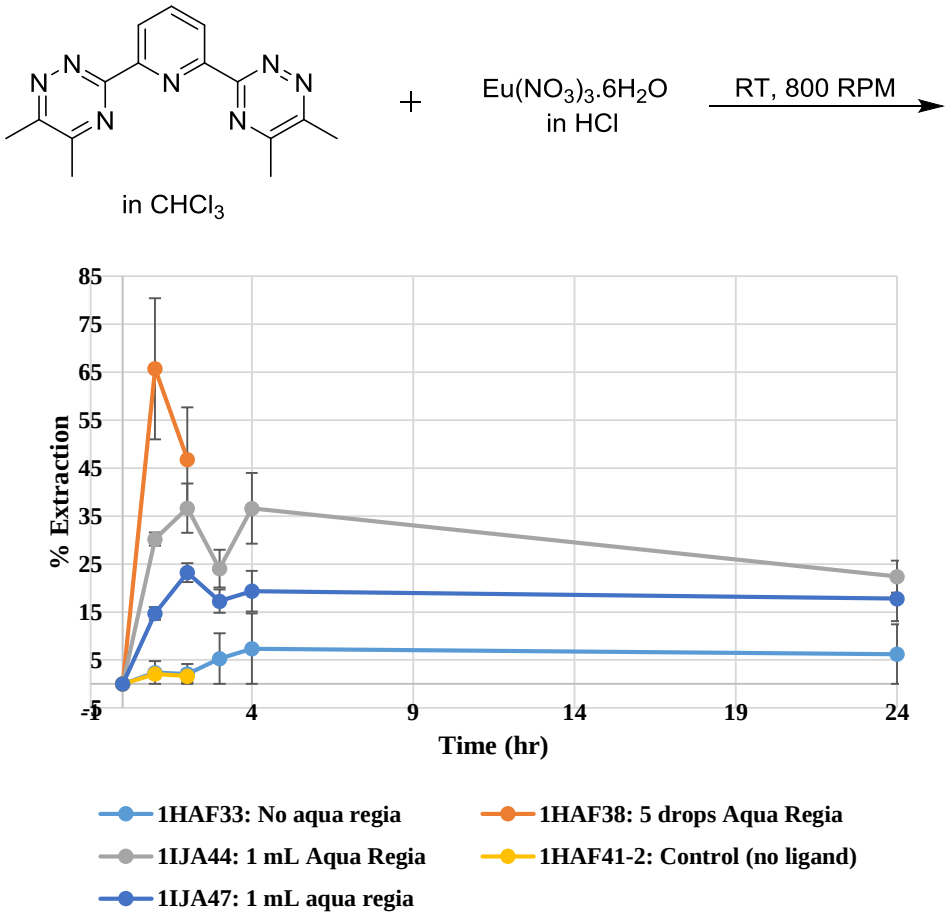

Scheme 6: Extraction of 0.002 M Eu in 0.001 M HCl by 0.05 M Me₄-BTP in $CHCl_3$

The selectivity of Me₄-BTP for Eu over Y was also explored (Scheme 7). Computational models had shown that Me₄-BTP would preferentially bind to Eu^{3+}, which has an ionic radius of 1.07 Å, over Y^{3+}, which has the smallest ionic radius of 1.04 Å. In an extraction with a mixture of Eu and Y, Scheme 4 shows that Me₄-BTP was not selective for Eu over Y. The distribution ratio of Eu, as calculated by Equation 2, for the experiment at 3 hours is $D_{Eu} = 0.19$ and the distribution ratio of Y is $D_Y = 0.13$.

$$D_A = [M_A]_{org}/[M_A]_{aq}$$

Equation 2

This gives a selectivity fraction of SF = 1.48, meaning that there was almost equal selectivity for the two REEs, despite the computational predictions. Due to the added danger of a

sample preparation with aqua regia, the consistently high RSDs, some negative extraction values from the ICP-OES, and the poor selectivity, we decided to shift focus from Me_4-BTP to BTP as a selective extracting agent for Eu.

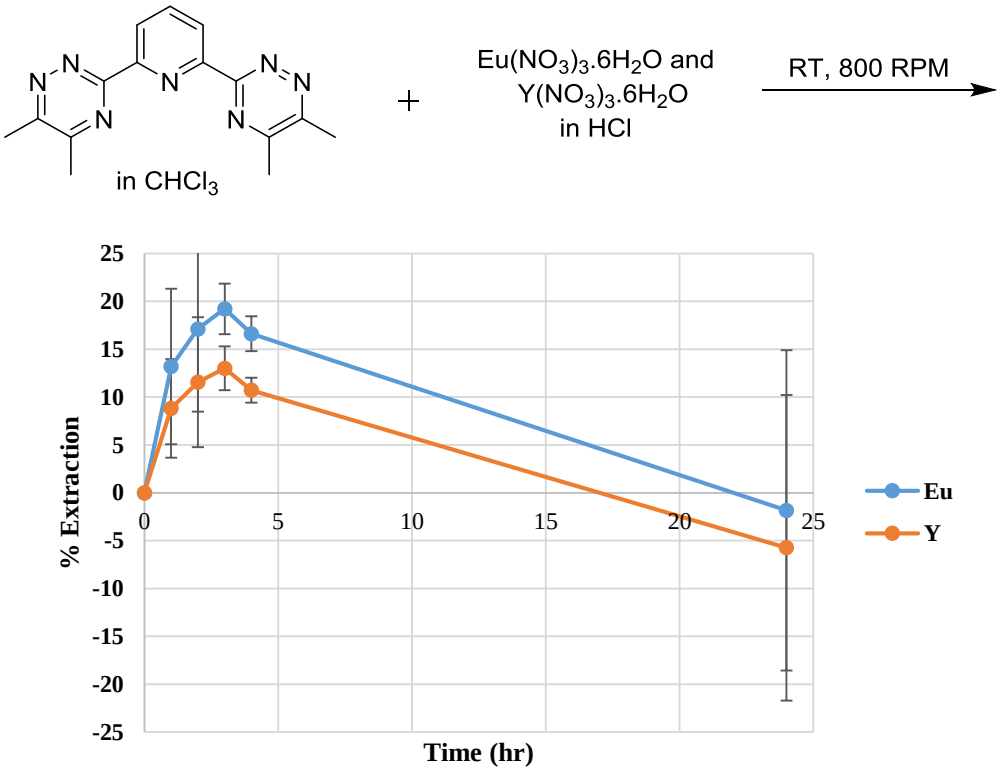

Scheme 7:Extraction of 0.002 M Eu and 0.002 M Y in 0.001 M HCl by 0.05 Me_4-BTP in $CHCl_3$.

2.4 Characterization of BTP-REE Complexes through ESI-MS

2.4.1 Europium and BTP Complexes

To identify BTP-Eu complexes, peaks that showed the characteristic isotopic splitting pattern for Eu, shown in Figure 5, were investigated.

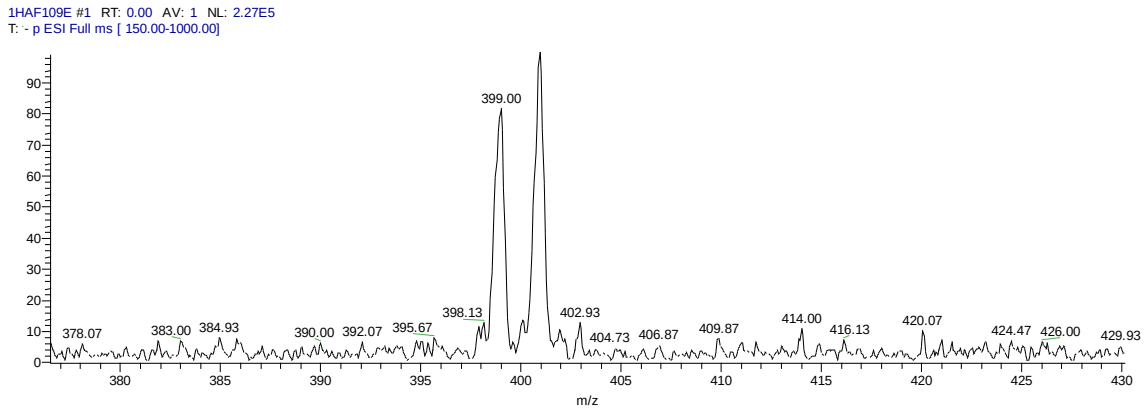

Figure 5: Isotopic splitting pattern of Eu. Conditions: 2.2×10^{-5} M $Eu(NO_3)_3.6H_2O$ in 0.004 M HNO_3 and MeOH in the negative ion mode.

Peaks indicating BTP-Eu complexes were found in the positive mode at 452 m/z and 687 m/z (Figure 6). We predicted that these peaks were $[Eu(BTP)(MeO)_2]^+$ at 452 m/z and $[Eu(BTP)_2(MeO)_2]^+$ at 687 m/z.

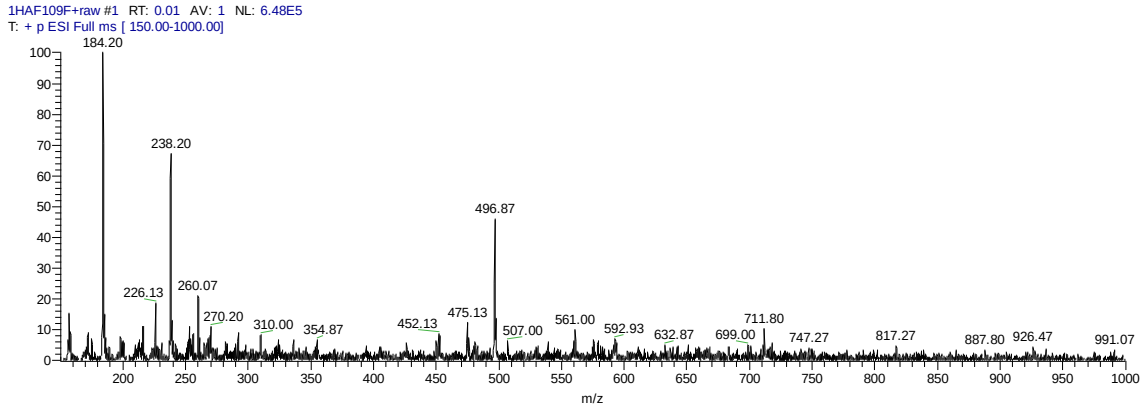

Figure 6: ESI-MS positive ion mode spectra of Eu and BTP complexes. Conditions: 2.2×10^{-5} M $Eu(NO_3)_3.6H_2O$ and 5.9×10^{-4} M BTP in 0.004 M HNO_3 and MeOH.

The peak at 452 m/z was investigated through ESI-MS/MS (Figure 7). After increased ionization, a peak at 426 m/z showed up, which we predicted to be $[Eu(BTP)(OH)_2]^+$. This supported the prediction that 452 m/z was $[Eu(BTP)(MeO)_2]^+$ because we could see two methoxy groups (each with a mass to charge ratio of 31) fall off of the molecule, to be replaced by two hydroxy groups (each with a mass to charge ratio of 17).

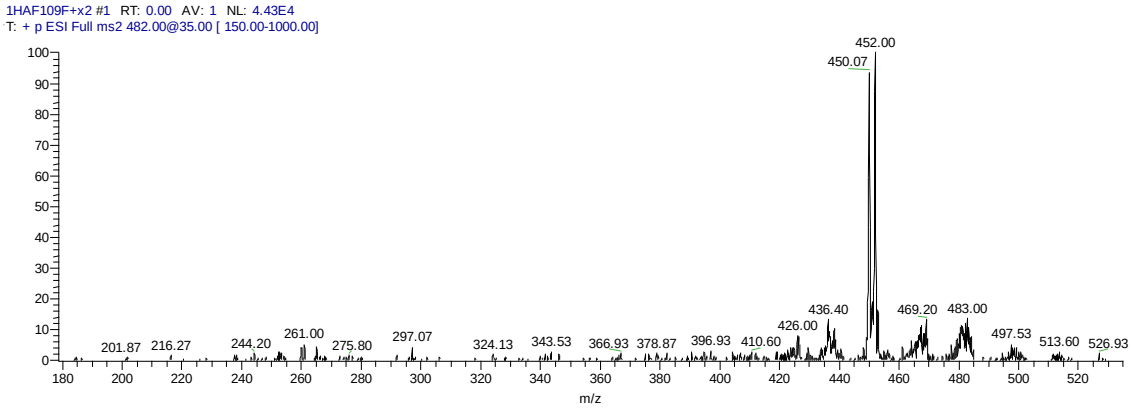

Figure 7: ESI-MS/MS in the positive ion mode of peak 452 m/z. Conditions: 2.2×10^{-5} M $Eu(NO_3)_3.6H_2O$ and 5.9×10^{-4} M BTP in 0.004 M HNO_3 and MeOH.

.

The peak at 687 m/z found through ESI-MS was investigated through ESI-MS/MS (Figure 8). After increased ionization, a peak at 512 m/z showed up, which we predicted to be $[Eu(BTP)(NO_3)_2]^+$. This supported the prediction that the complex at 687 m/z was $[Eu(BTP)_2(MeO)_2]^+$ because we saw a BTP ligand (with mass to charge ratio of 237) and nitrate groups (with mass to charge ratio of 62) fall off the molecule, and methoxy groups to bind.

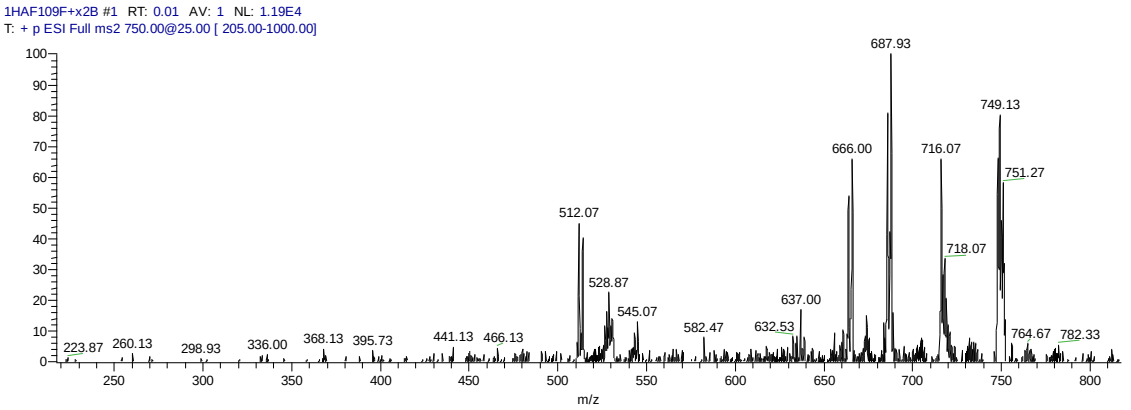

Figure 8: ESI-MS/MS in the positive ion mode of 687 m/z peak. Conditions: 2.2×10^{-5} M $Eu(NO_3)_3.6H_2O$ and 5.9×10^{-4} M BTP in 0.004 M HNO_3 and MeOH.

The peak at 512 m/z was investigated through ESI-MS/MS/MS (Figure 9). Further ionization revealed a peak at 481 m/z, which we predicted to be $[Eu(BTP)(NO_3)(MeO)]^+$. It also revealed a peak at 468 m/z which we predicted to be $[Eu(HBTP)(MeO)(OH)]^+$. This supported the

prediction that 512 m/z was $[Eu(BTP)(NO_3)_2]^+$ because we could see the nitrate groups falling off and methoxy and hydroxyl groups binding.

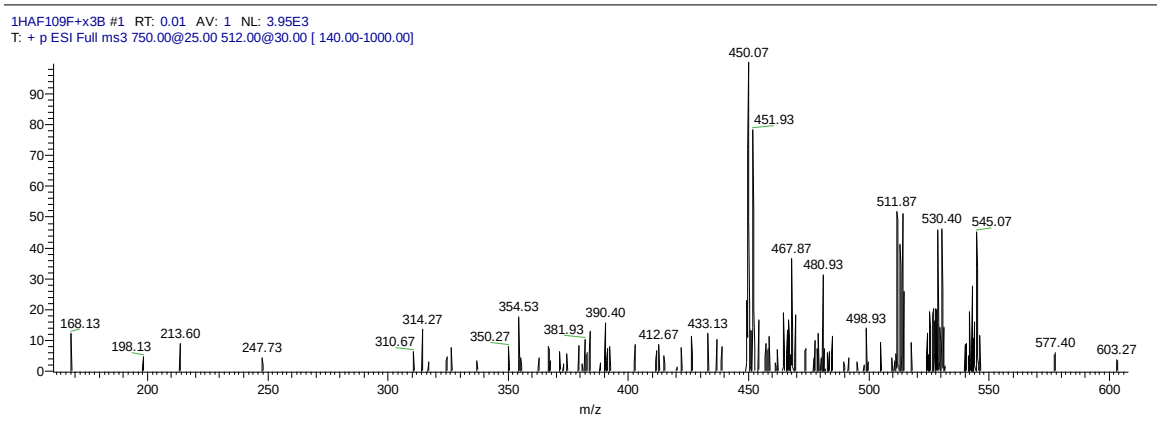

Figure 9: ESI-MS/MS/MS in the positive ion mode of peak 512 m/z. Conditions: 2.2×10^{-5} M $Eu(NO_3)_3.6H_2O$ and 5.9×10^{-4} M BTP in 0.004 M HNO_3 and MeOH.

This characterization through ESI-MS showed that Eu made complexes with either one or two BTP ligands and two other groups.

2.4.2 Dysprosium and BTP Complexes

To identify BTP-Dy complexes, peaks that showed the characteristic isotopic splitting pattern for Dy, shown in Figure 10, were investigated.

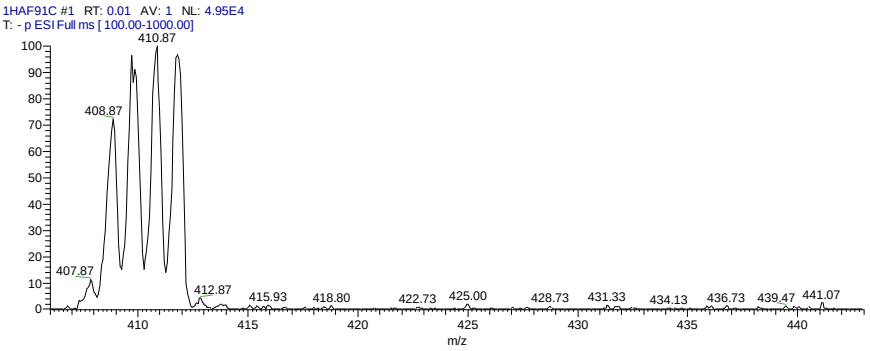

Figure 10: Isotopic splitting pattern of Dy in the negative ion mode. Conditions: 2.2×10^{-5} M $Dy(NO_3)_3.6H_2O$ in 0.004 M HNO_3 and MeOH.

A peak indicating a BTP-Dy complex was found in the positive mode at 761 m/z (Figure 11). We predicted that this peak was $[Dy(BTP)_2(NO_3)_2]^+$.

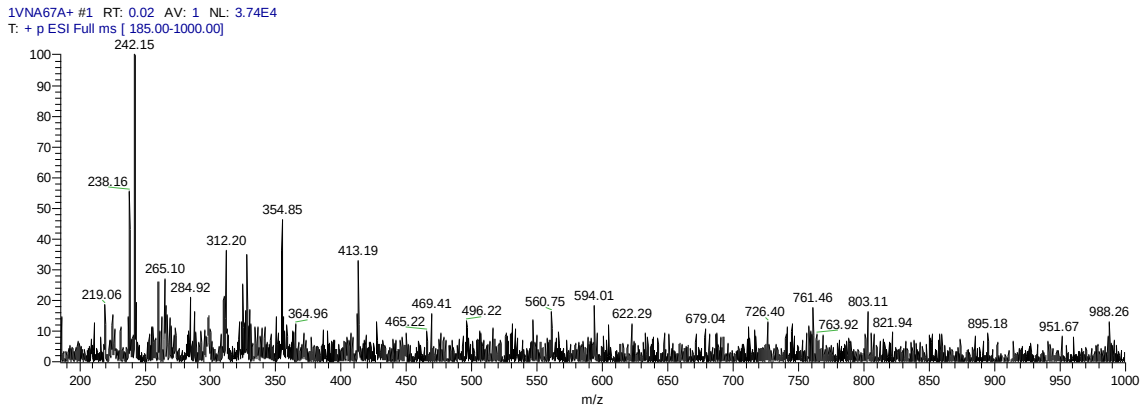

Figure 11: ESI-MS positive ion mode spectra of Dy and BTP complexes. Conditions: 2.2×10^{-5} M $Dy(NO_3)_3.6H_2O$ and 5.9×10^{-4} M BTP in 0.004 M HNO_3 and MeOH.

The peak at 761 m/z found through ESI-MS was investigated with ESI-MS/MS (Figure 12). After increased ionization, a peak at 524 m/z showed up, which we predicted to be $[Dy(BTP)(NO_3)_2]^+$. This supported the prediction that 761 m/z was $[Dy(BTP)_2(NO_3)_2]^+$ because we could see a BTP ligand fall off. We also found a peak at 677 m/z which had the isotopic splitting pattern, however with the mass to charge ratios of the ions available and the BTP ligand a complex could not be formed with this value. Therefore we decided to stop investigating this peak.

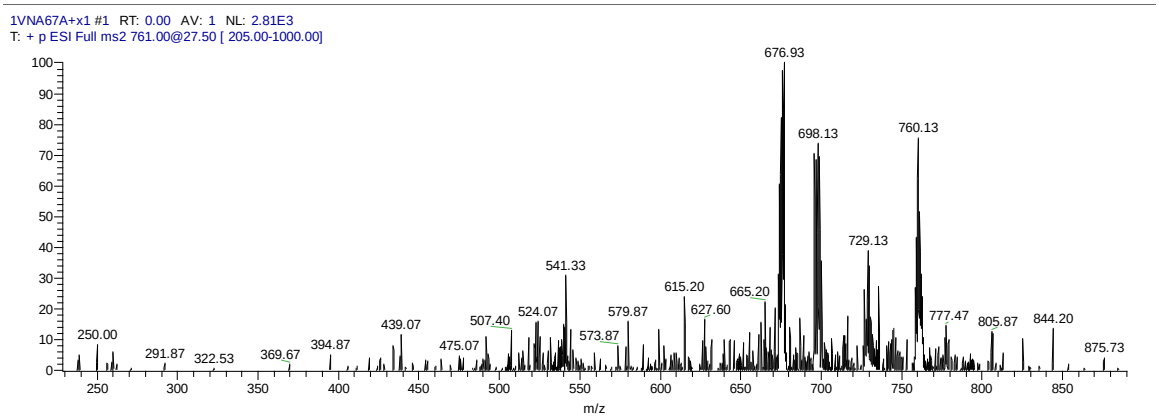

Figure 12: ESI-MS/MS in the positive ion mode of peak 761 m/z. Conditions: 2.2×10^{-5} M $Dy(NO_3)_3.6H_2O$ and 5.9×10^{-4} M BTP in 0.004 M HNO_3 and MeOH.

This characterization through ESI-MS showed that Dy made complexes with two BTP ligands and two nitrates.

2.4.3 Erbium and BTP Complexes

To identify Er complexes, peaks that showed the isotopic splitting pattern for Er, shown in Figure 13, were investigated.

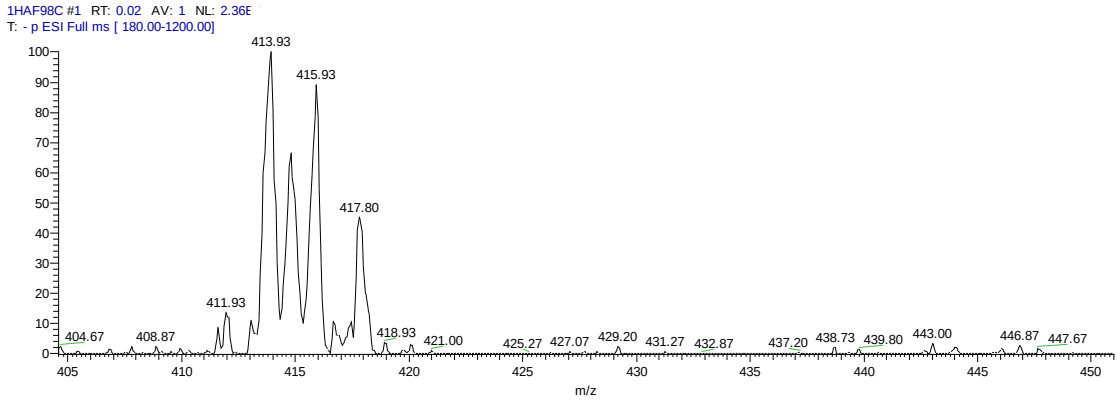

Figure 13: Isotopic splitting pattern of Er in the negative ion mode. Conditions: 2.2×10^{-5} M $Er(NO_3)_3.6H_2O$ in 0.004 M HNO_3 and MeOH..

Peaks indicating Er complexes were found in the positive mode at 496 m/z and 765 m/z (Figure 14). We predicted that the peak at 496 m/z was either $[Na(BTP)_2]^+$ or $[Er(BTP)(NO_3)(OMe)]^+$. We predicted that the peak at 765 m/z was $[Er(BTP)_2(NO_3)_2]^+$.

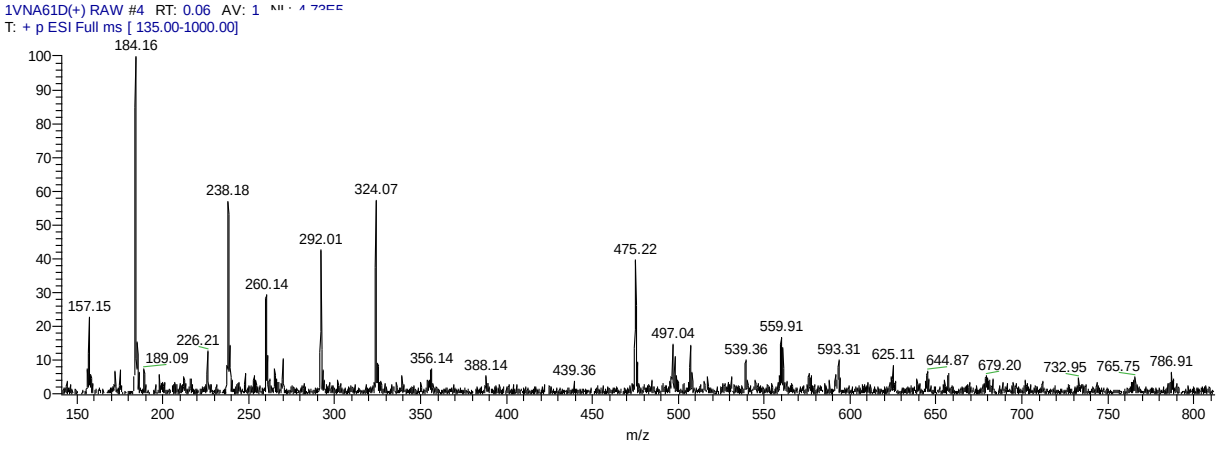

Figure 14: ESI-MS spectra in the postive mode of a solution of BTP and Er. Conditions: 2.2×10^{-5} M $Er(NO_3)_3.6H_2O$ and 5.9×10^{-4} M BTP in 0.004 M HNO_3 and MeOH.

The peak at 496 m/z was investigated through ESI-MS/MS (Figure 15). After increased ionization, a peak at 484 m/z which had the Er isotopic splitting pattern showed up, which we

predicted to be $[Er(BTP)(NO_2)(OH)]^+$. This supported the prediction that 496 m/z was $[Er(BTP)(NO_3)(MeO)]^+$ because we could see a methoxy group fall off of the molecule, to be replaced by an hydroxy group. However, we also found a peak at 260 m/z which did not show the Er isotopic splitting pattern, which we predicted to be $[NaBTP]^+$, showing that the peak at 496 m/z could have recorded both $[Er(BTP)(NO_3)(MeO)]^+$ and $[Na(BTP)_2]^+$.

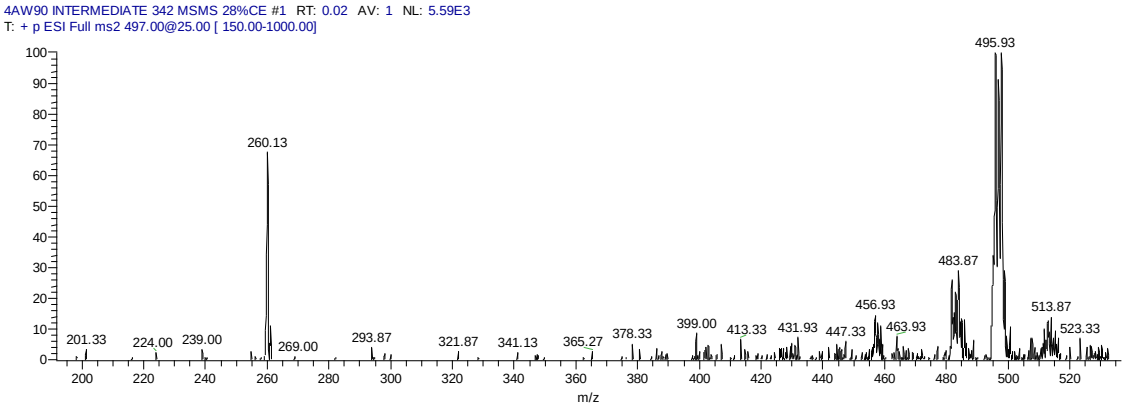

Figure 15: ESI-MS/MS in the positive ion mode of peak 452 m/z. Conditions: 2.2×10^{-5} M $Er(NO_3)_3.6H_2O$ and 5.9×10^{-4} M BTP in 0.004 M HNO_3 and MeOH.

The peak at 765 m/z found through ESI-MS was investigated through ESI-MS/MS (Figure 16). After increased ionization, a peak at 528 m/z showed up, displaying the isotopic splitting pattern of Er, which we predicted to be $[Er(BTP)(NO_3)_2]^+$. This supported the prediction that the complex at 765 m/z was $[Er(BTP)_2(NO_3)_2]^+$ because we saw a BTP ligand fall off the molecule. A peak at 702 m/z also showed up, which we predicted to be $[Er(BTP)(MeO)_2]^+$. This supported the prediction that the complex at 765 m/z $[Er(BTP)_2(NO_3)_2]^+$ because we saw the two nitrate groups fall off and two methoxy groups bind.

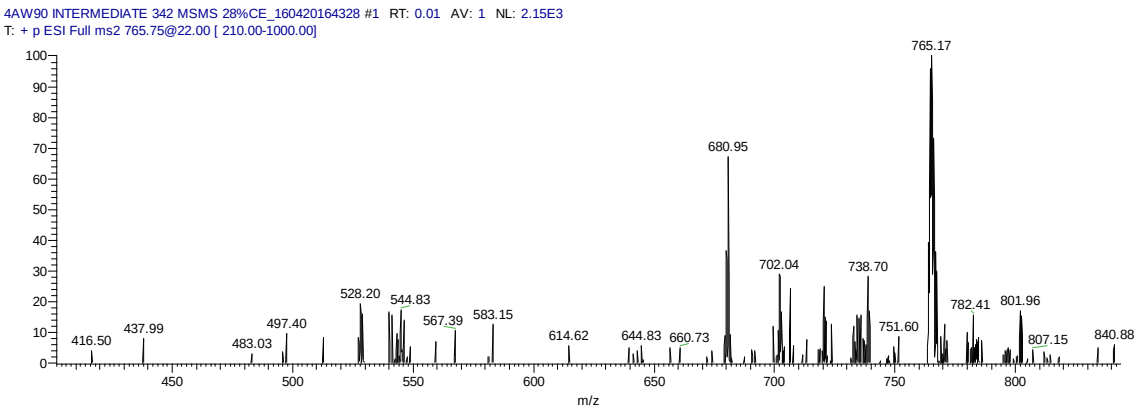

Figure 16: ESI-MS/MS in the positive ion mode of peak 765 m/z. Conditions: 2.2×10^{-5} M $Er(NO_3)_3.6H_2O$ and 5.9×10^{-4} M BTP in 0.004 M HNO_3 and MeOH.

Similar to Eu, the characterization of Er and BTP complexes through ESI-MS showed that Er made bonded with either one or two BTP ligands and two other groups.

2.4.4 Gadolinium and BTP Complexes

To identify Gd complexes, peaks that showed the isotopic splitting pattern for Gd, shown in Figure 17, were investigated.

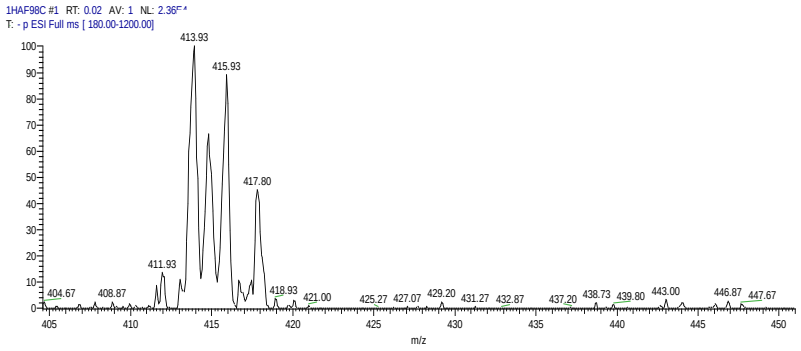

Figure 17: Isotopic splitting pattern of Gd in the negative ion mode. Conditions: 2.2×10^{-5} M $Gd(NO_3)_3.6H_2O$ in 0.004 M HNO_3 and MeOH..

Peaks indicating Gd complexes were found in the positive mode at 488 m/z and 659 m/z and 756 m/z (Figure 18). We predicted that the peak at 488 m/z was $[Gd(BTP)(NO_3)(OMe)]^+$, that the peak at 659 m/z was $[Gd(BTP)(NO_3)_3(OMe)Na_2]^+$, and that the peak at 756 m/z was $[Gd(BTP)_2(NO_3)_2]^+$.

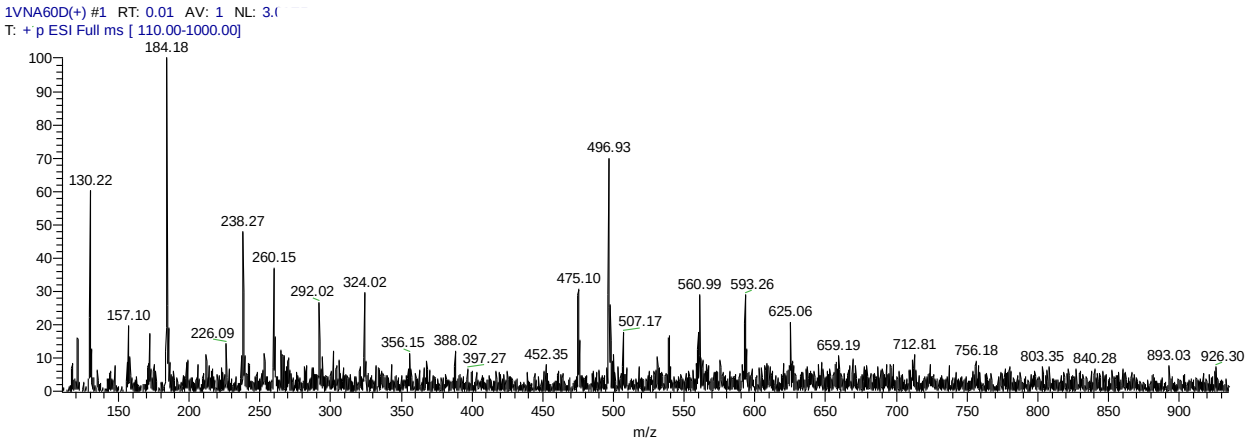

Figure 18: ESI-MS spectra in the postive mode of a solution of BTP and Gd. Conditions: 2.2×10^{-5} M $Gd(NO_3)_3.6H_2O$ and 5.9×10^{-4} M BTP in 0.004 M HNO_3 and MeOH.

The peak at 488 m/z was investigated through ESI-MS/MS (Figure 19). After increased ionization, a peak at 474 m/z which had the Gd isotopic splitting pattern showed up, which we predicted to be $[Gd(BTP)(NO_2)(OH)]^+$. This supported the prediction that 488 m/z was $[Gd(BTP)(NO_3)(MeO)]^+$ because we could see a methoxy group fall off of the molecule, to be replaced by an hydroxy group. We also found a very small peak at 252 m/z which could be $[Gd(NO_3)(OMe)]^+$ because it has a mass to charge ration 237 less than the peak at 488 m/z, and we also saw a peak appear at 238 m/z which indicates the presence of $[HBTP]^+$. However, the peak at 252 m/z was too small to see if it had the Gd isotopic splitting pattern.

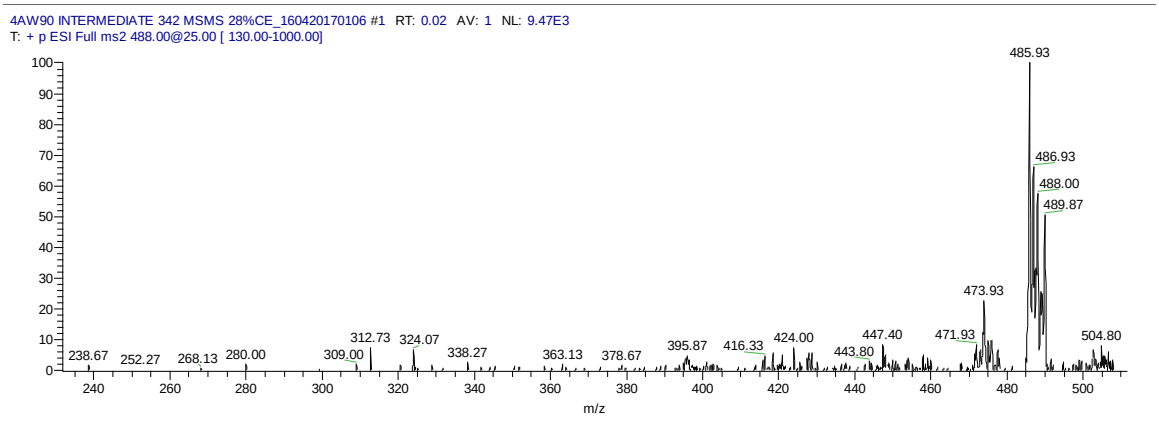

Figure 19: ESI-MS/MS in the positive mode of peak 488 m/z. Conditions: 2.2×10^{-5} M $Gd(NO_3)_3.6H_2O$ and 5.9×10^{-4} M BTP in 0.004 M HNO_3 and MeOH.

The peak at 659 m/z found through ESI-MS was investigated through ESI-MS/MS (Figure 20). After increased ionization, a peak at 628 m/z showed up, displaying the isotopic splitting pattern of Gd, which we predicted to be $[Gd(Na_2BTP)(NO_3)_2(OMe)_2]^+$. This supported the prediction that the complex at 659 m/z was $[Gd(Na_2BTP)(NO_3)_3(OMe)]^+$ because we saw a nitrate group fall off and a methoxy group bind.

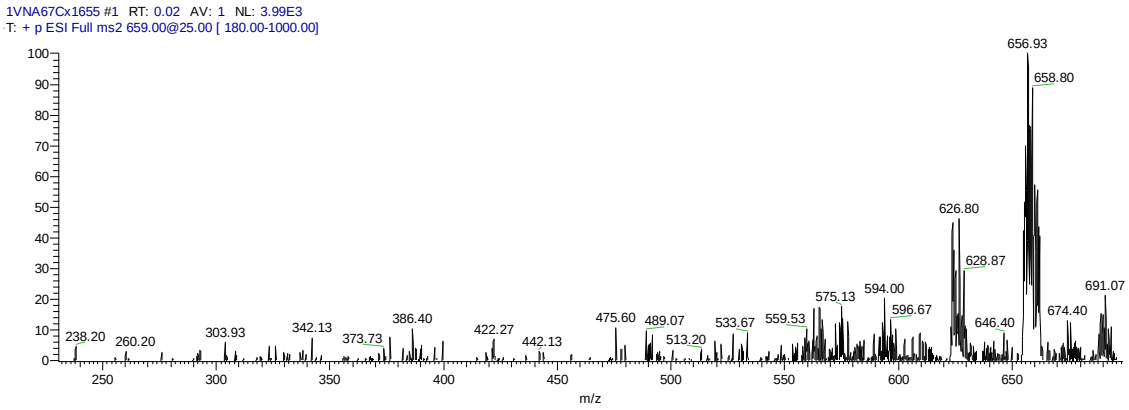

Figure 20: ESI-MS/MS in the positive ion mode of 659 m/z peak. Conditions: 2.2×10^{-5} M $Gd(NO_3)_3.6H_2O$ and 5.9×10^{-4} M BTP in 0.004 M HNO_3 and MeOH.

The peak at 756 m/z found through ESI-MS was investigated through ESI-MS/MS (Figure 21). After increased ionization, a peak at 519 m/z showed up, displaying the isotopic splitting pattern of Gd, which we predicted to be $[Gd(BTP)(NO_3)_2]^+$. We also saw a 238 m/z peak appear which shows $[HBTP]^+$ being formed. This supported the prediction that the complex at 756 m/z was $[Gd(BTP)_2(NO_3)_2]^+$ because we saw a BTP ligand fall off. We also saw a peak at 725 m/z which we predict to be $[Gd(BTP)_2(NO_3)(MeO)]^+$. This supported the prediction that the complex at 756 m/z was $[Gd(BTP)_2(NO_3)_2]^+$ because we saw a nitrate group fall off and a methoxy group bind. Finally we saw a peak at 694 m/z which we predicted to be $[Gd(BTP)_2(MeO)_2]^+$. This supported the prediction that the complex at 756 was $[Gd(BTP)_2(NO_3)_2]^+$ because we saw the nitrate groups fall off and two methoxy groups bind.

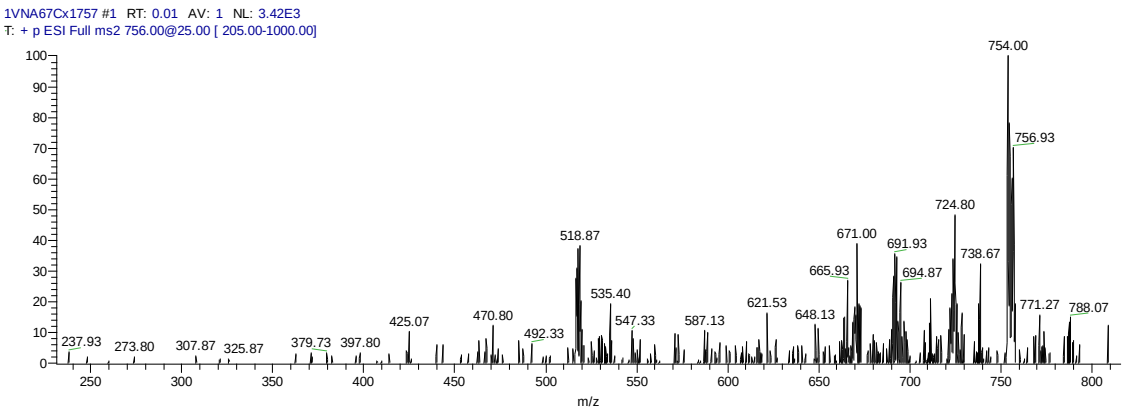

Figure 21: ESI-MS/MS in the positive ion mode of peak 756 m/z. Conditions: 2.2×10^{-5} M $Gd(NO_3)_3.6H_2O$ and 5.9×10^{-4} M BTP in 0.004 M HNO_3 and MeOH.

Similar to Eu, the characterization of Gd and BTP complexes through ESI-MS showed that Er made bonds with either one or two BTP ligands and two other groups.

2.5 Extraction with BTP

Computational models done by Kathleen Field supported the hypothesis that BTP would selectively extract Eu as mentioned in section 1.11. So, the efficacy of BTP as an extractant, and its selectivity for Eu was tested under a variety of conditions. Several aspects of the extraction had to be optimized, starting with the acid used to dissolve the REE nitrate.

2.5.1 Acid Studies

The acid is very important in an extraction. The anion from the acid can bind with the metal in the metal-ligand complex and help the REE move into the organic phase, but too much H^+ from the acid will protonate the extractant at the metal binding site. The best acid and concentration had to be determined for the best possible extraction. Scheme 8 the extraction of Eu under different acidic conditions. The best condition may appear to be 0.001 M H_2SO_4, however the reaction formed a strong emulsion which didn't separate, in some cases, in over 24 hours. The high extraction, and the high RSDs, could be due to Eu in the organic phase that had gone through the aqueous sample preparation for the ICP-OES. The best condition is 0.001 M HCl, followed by 0.001 M HNO_3. Both acids were continued to be used in later extractions.

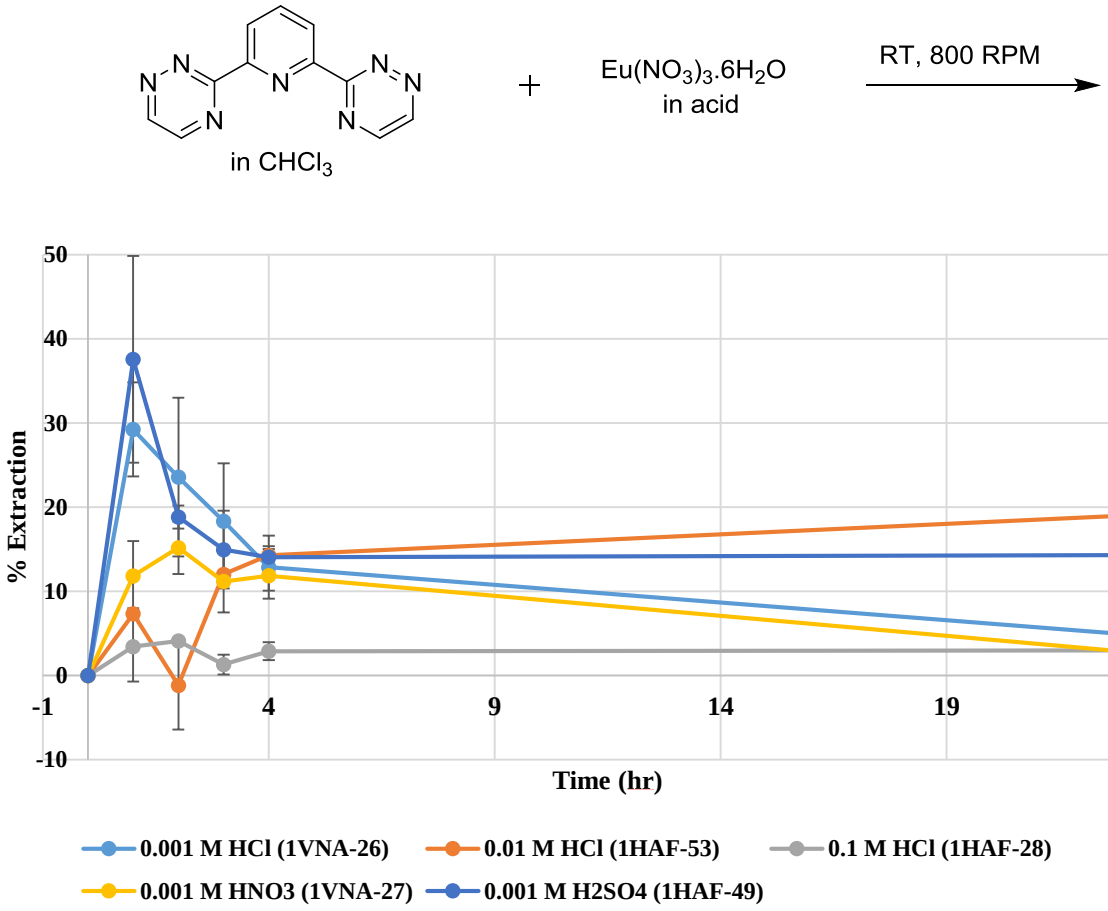

Scheme 8: Extraction of 0.002 M Eu in varying acids and concentrations by 0.05 M BTP in 19:1 $CHCl_3$:Oct.

2.5.2 Metal Studies

Next, BTP was used to extract several of the rare earth elements to determine which REE it had the greatest affinity for. The REEs were extracted individually, and not in a mixture. Scheme 9 shows that BTP was not selective for any of the REEs tested. The RSDs were also much higher than 10%. Because the BTP did not seem to be selective for Eu, despite the computational model, we decided to add salts to help improve the extractions.

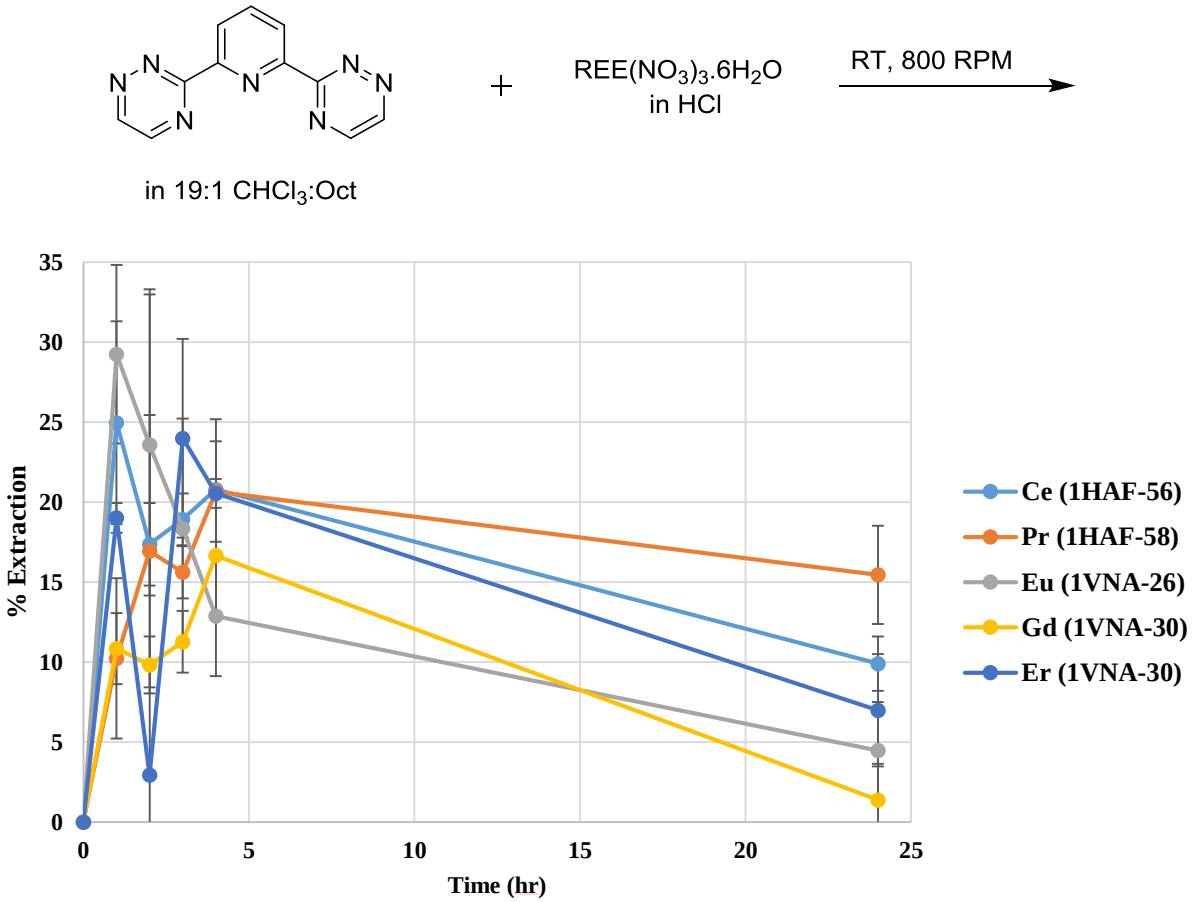

Scheme 9: Extraction of 0.002 M REE in 0.001 M HCl by 0.05 M BTP in 19:1 $CHCl_3$:Oct.

2.5.3 Salt Studies

After determining which acid worked best with BTP, it was important to consider if other additives would help improve the extraction yields. Eu has nine coordination sites available when forming a complex. Since it is thought that BTP coordinates to Eu twice, each taking up two coordination sites, there are still give open coordination sites for the Eu to bind. This opened up the idea to include different salts such as potassium acetate or sodium acetate into the reaction vessel. There were three main cations (lithium, sodium, potassium) and several other anions tested to determine which salt, if any, improves the percent of REE extracted by BTP.

Sodium cation and its counter ion were the first salts tested. The sodium was paired with nitrate, nitrite, chlorine, bromine, and acetate groups as shown in Scheme 10. This graph also included some extractions run in HNO_3 which support the previous data of lower extraction

percentages when compared to HCl. However, when comparing the salts, the addition of sodium acetate in HCl showed the largest positive increase over the baseline extraction of Eu in HCl with no salts. The extraction percentages increased from a maximum of 29% to a maximum of 40%. The sodium acetate extraction had very small RSDs compared to the other experiments. Furthermore, other salts containing sodium and an anion did not increase the overall yields of these extractions.

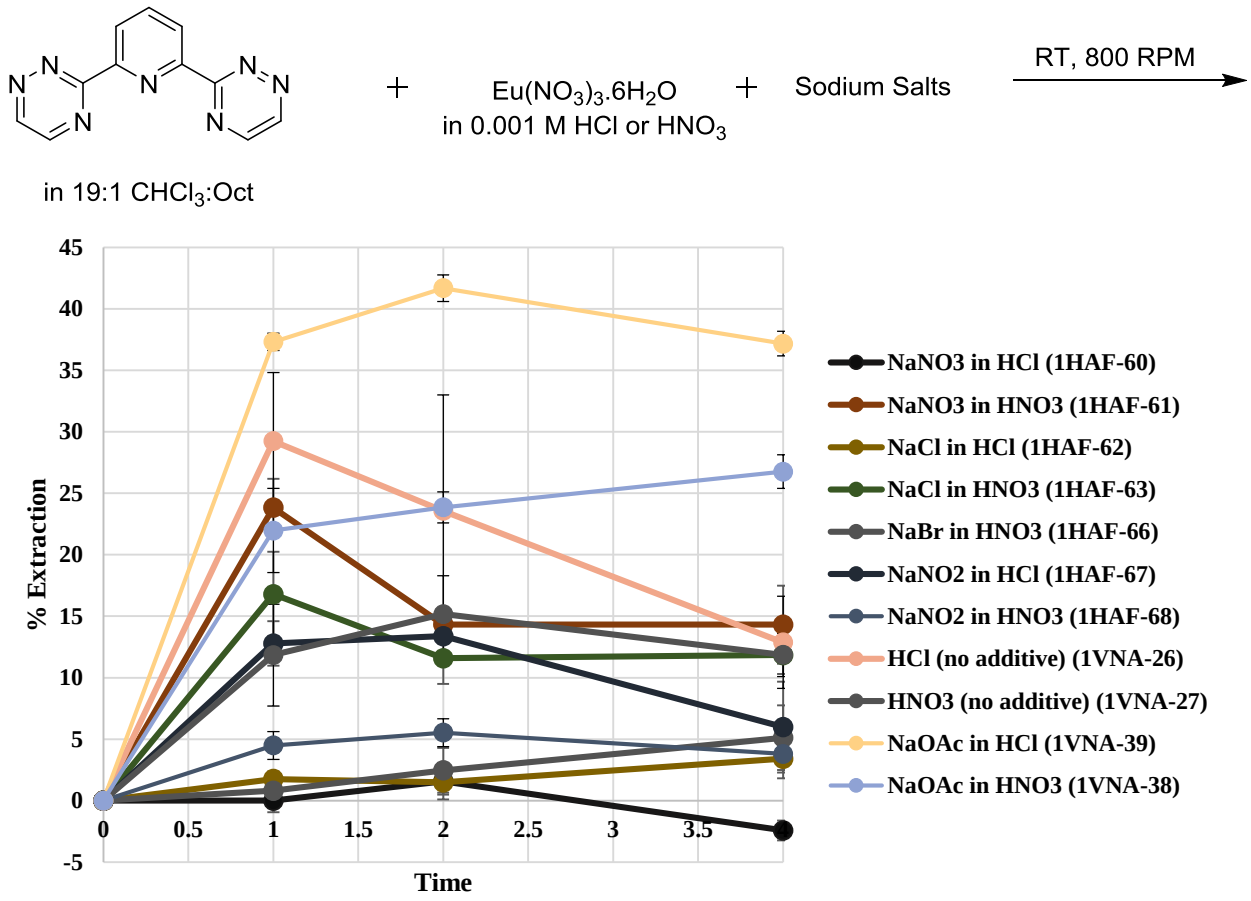

Scheme 10: Extraction of 0.002 M Eu and 0.006 M Na salt in 0.001 M HCl or 0.001 M HNO_3 by 0.05 M BTP in 19:1 $CHCl_3$:Oct.

After trying several different sodium salts, the cation was changed to potassium. Scheme 11 looked at potassium nitrates and potassium acetates in both HCl and HNO_3. In this set of experiments, the larger cation did not improve the overall extraction in the optimized HCl conditions. The maximum 29% yield from the HCl extraction with no additives went down to a maximum of 17% with potassium acetate. This did not do as well as the smaller ionic radius cation

of sodium. This led us to believe that a smaller ionic radius could potentially produce even better yields.

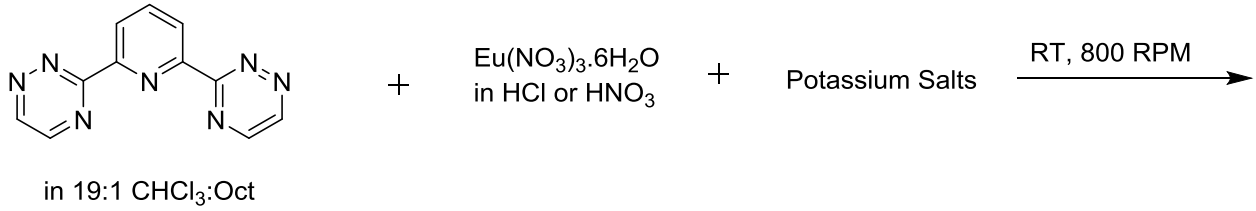

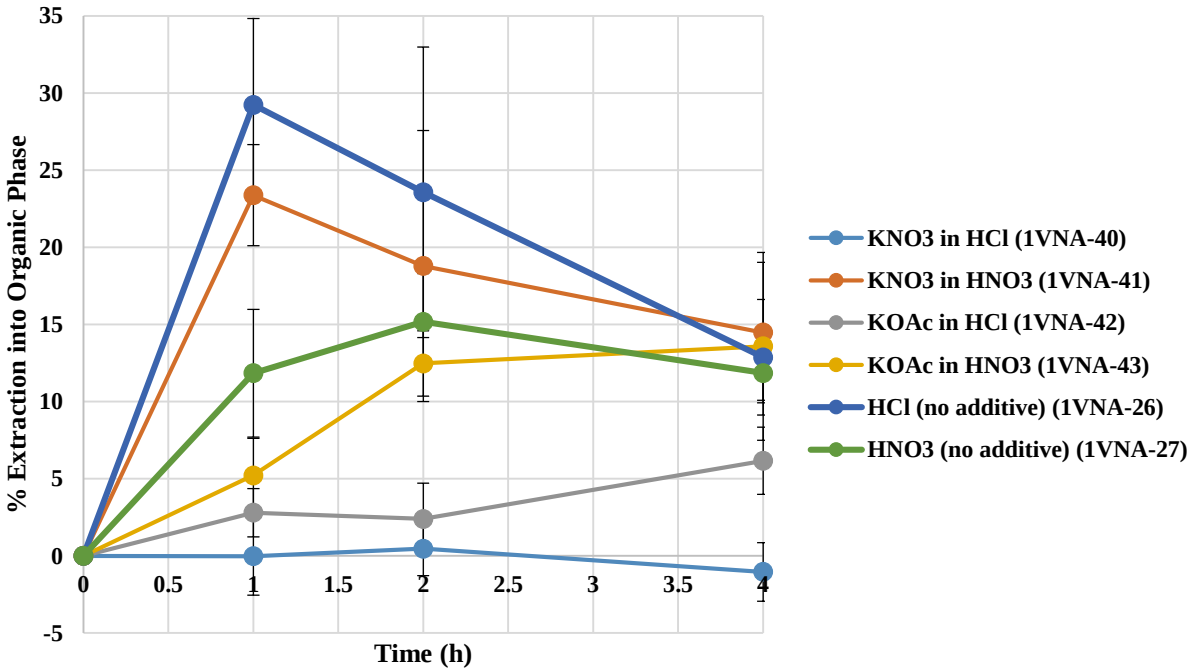

Scheme 11: Extraction of 0.002 M Eu and 0.006 M K salt in 0.001 M HCl or 0.001 M HNO_3 by 0.05 M BTP in 19:1 $CHCl_3$:Oct..

The last cation researched was Li^+ in lithium acetate. Scheme 12 shows the resulting extraction percentages at different time points in HCl. The lithium ion ended up producing a yield above 40% under the HCl conditions. However, this experiment had higher error bars than desired and more testing would need to be conducted to support the hypothesis that a smaller counter-cation would be best suited for coordinated at the last three coordination sites of Eu.

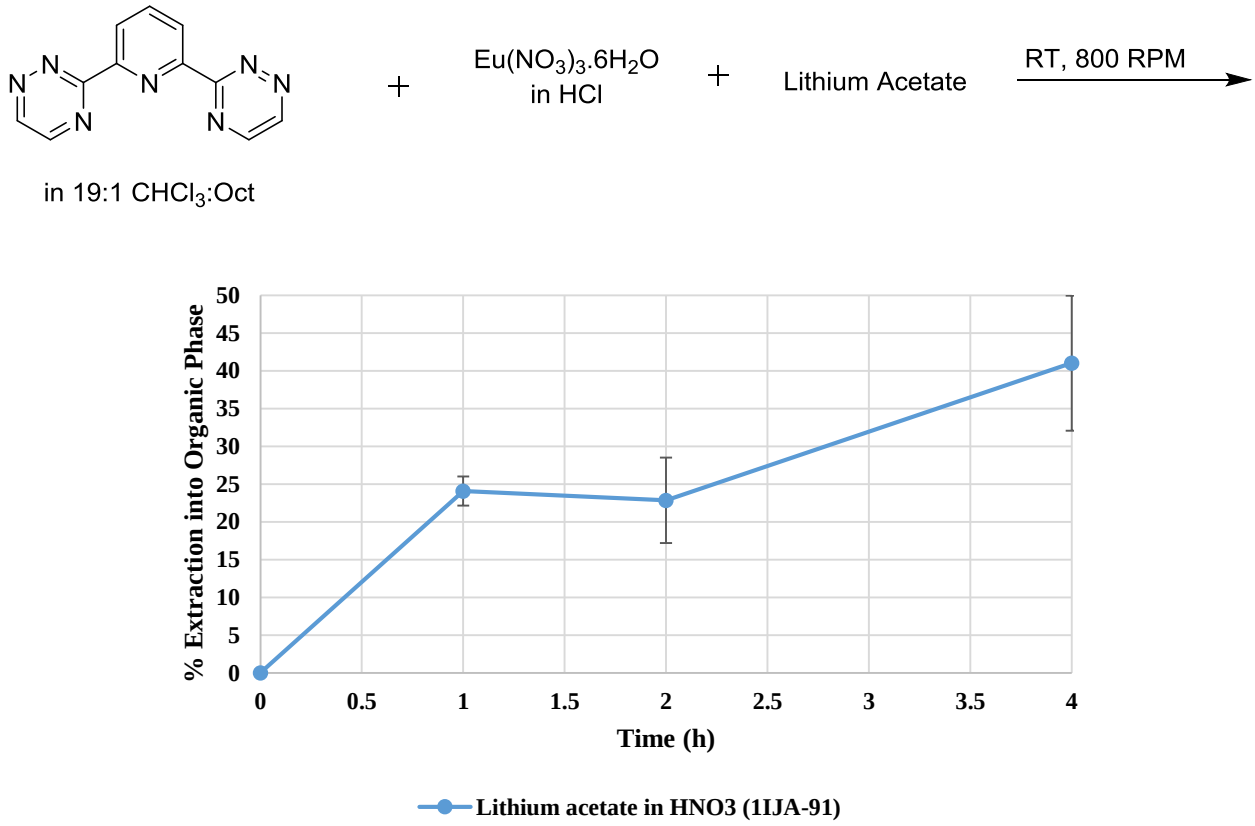

Scheme 12: Extraction of 0.002 M Eu and 0.006 M LiOAc in 0.001 M HNO_3 by 0.05 M BTP in 19:1 $CHCl_3$:Oct.

2.6 BTP Efficacy

So far in the investigation, we have not found that BTP selectively extracts Eu, despite predictions by our computational models. The highest extraction of Eu was obtained with 0.002 M $Eu(NO_3)_3 \cdot 6H_2O$ and 0.006 M sodium acetate in 0.001 M HCl and 0.05 M BTP in 19:1 $CHCl_3$:Oct, and had a distribution ratio of $D_{Eu} = 0.42$. This means that with the best conditions, less than half of the Eu was extracted into the organic phase. Neither was the BTP selective for Eu. Before including salts in the extraction, BTP was binding with all of the REEs. However, future work optimizing extractions through the use of different salts and their concentrations may help the BTP ligand to extract more Eu and become more selective for it.

3.0 Conclusion

At the start of the project the initial hypothesis was that BTP and BTP derivatives were capable of "fitting" around a particular metal based on ionic radii. Normally, as the bond length shortens, the stability increases and thus the binding potential will increase. However, the unusual trend for lanthanide series when binding to the BTP derivatives suggested that these ligands actually "fit" better for certain metals. This began the idea of finding optimal ligands capable of extracting individual rare earth metals starting BTP or BTP derivatives. This initial hypothesis was supported by the computational work done by Kathleen D. Field which showed BTP was more likely to complex with Eu than the other REEs.

Using this knowledge, synthesis of BTP was conducted and optimized over the course of this project. New solvent systems were developed and certain reactions conditions were optimized in an effort to achieve quality BTP synthesis. Me_4-BTP was also synthesized in the attempt to produce a selective ligand. Due to complications when analyzing this ligand, we decided to shift focus back to BTP in order to continue project progression. Several variables were changed, one at a time, to optimize the extraction by BTP starting with acid type, acid concentration, and different salt additives used during the liquid-liquid extraction. However, the extraction of Eu into the organic phase remained poor with a maximum extraction percentage of 42%.

Despite the lower extraction percentages, ligand-REE complexes formed, allowing them to be analyzed to better understand the way our main extractant, BTP, was complexing around a particular REE. The analysis by ESI-MS and ESI-MS/MS gave insight to the potential complexes formed between BTP and REE's. Generally, two BTP's were complexed to the REE, balanced out by counter ions in solution. Understanding how these BTP-REE complexes formed gave insight to the number of coordination sights available to which salt additives can coordinate. This information could then be used to further optimization of extractions.

It was important to understand that the computational method, while not always perfect, lead the project down a possible road for finding highly selective extractants for REE such as Eu. Looking at BTP derivatives and their ability to bind to these rare earth elements on their own through Gaussian gave insight on the binding potential in a solution containing which only REE and extractant. This caveat of the modeling system falls short when predicting the selectivity of the extractant when selecting for a particular REE within a mixture. Through our experiments, the

selectivity of BTP for Eu over other REE was determined to be lower than anticipated. Despite our initial hypothesis based on the work done by Gesit et. al.[22] the selectivity of BTP was not as great as expected under current extraction conditions. In order to achieve this selective and sustainable separation of REE, the reaction and its reagents require further optimization. This could include focusing on a different ligand or adding different functional groups to BTP.

Overall, the future for this area of research is promising. Ideally, a unique ligand will exist for each individual REE with the capability to selectively separate out that particular REE from a mixture. Therefore seventeen different extractants would go through this process of computational analysis, synthesis, characterization, and liquid-liquid extraction. Each of these steps would undergo intensive optimization in order to achieve the best possible results when extraction REEs on a large scale. Luckily, the variety of BTP derivatives which can be synthesized will prove helpful when trying to design new extractants for different REEs. Through continued optimization, these extractions can eventually reach higher percentages as well as higher selectivity.

4.0 Future Directions

The pursuit of highly selective ligands is still a challenge in this project. The high similarity between the REEs chemical properties, physical properties, and ionic radii continue to make designing a highly selective extractant difficult. However, this project has a promising future with the new directions this project can be taken. Through the synthesis of new ligands, new extractants may prove more selective. By continuing the cyclical approach of computation, synthesis, characterization, and extraction, exploring molecules such as BTP-Cl_4 or 6,6'-(4-phenylpyridine-2,6-diyl)bis(3-chloropyridazine) could lead to the discovery of a highly selective ligand. In addition to the use of Gaussian to computationally predict potential extractants, ESI-MS can be used as supporting evidence to show that BTP, or other potential ligands, complexes to the metal. Furthermore, the continuation of optimization will further enhance the extracting potential of both current and future ligands. These optimizations can continue mostly in the additions of various salts for extractions as well as optimizing the solvent system for BTP. All of these actions and experiments will benefit the overall extraction potential of all ligands in an effort to produce a highly selective.

5.0 Experimental Section

5.1 General Procedures: Techniques, Solvents, and Chemicals

All reactions were performed in air at room temperature and all solvents used were technical grade. All rare earth oxides were obtained commercially in the +3 oxidation state as nitrate hydrates, and stored in a desiccator cabinet. All acid concentrations were made through dilutions from 4 molar stock solutions. All BTP, Me_4-BTP, and rare earth solutions were used in extractions the same day they were made. All reagents were purchased and used without additional purification. Ultra High Purity (UHP) water was obtained from Millipore Q Academic purification system.

5.2 Synthesis of Ligands

5.2.1 NMR

^{1}H NMR was used to determine the presence and purity of synthesized organic ligands. ^{1}H NMR spectra were recorded on a Bruker BioSpin AG 500 MHz Advance III Digital NMR spectrometer. $CDCl_3$ and DMSO-*d*6 were used as solvents. NMR tubes with BTP products were placed in a water sonication bath to break up BTP particles and create a uniform suspension. The shift of the standard signal in $CDCl_3$ was calibrated to 7.26 ppm, while DMSO-*d*6 was calibrated to 2.50 ppm. The following abbreviations are used for the description of the signals for ligand products: *s*: singlet, *d*: doublet, *t*: triplet.

5.2.2 GC

Experiments can be found in 1HAF-93.

GC analyses were performed on an Agilent 7890A Series GC equipped with FID detector, an Agilent HP-5 capillary column (length 30m, diameter 0.32 mm, film thickness 0.25 μm), and a 7693A auto injector module. Yields were calculated by calibrating prepared samples and phenyl bromide standard to the response of the instrument. These prepared samples were 1 ml solutions of BTP in 1:1 $CHCl_3$:MeOH at concentrations of 0 M, 0.005 M, 0.015 M, 0.025 M, 0.035 M, 0.05 M, and 0.075 M (1HAF-93). PhBr (10 μL, 0.095 mmol) was added to each calibration solution as

an internal standard. Each prepared sample produced a BTP peak and a phenyl bromide peak on the GC chromatogram. Figure 22 shows that the ratio of the area of the BTP peak to the area of the phenyl bromide peak could be plotted against the ratio of mmol of BTP to mmol of phenyl bromide, to obtain a calibration curve. Equation 1 uses the calibration curve to calculate the number of mmol of BTP in a sample.

$$mmol\ BTP = 1.8272 \times \frac{Area_{sample}}{Area_{PhBr}} \times 0.095\ mmol\ PhBr$$

Equation 2

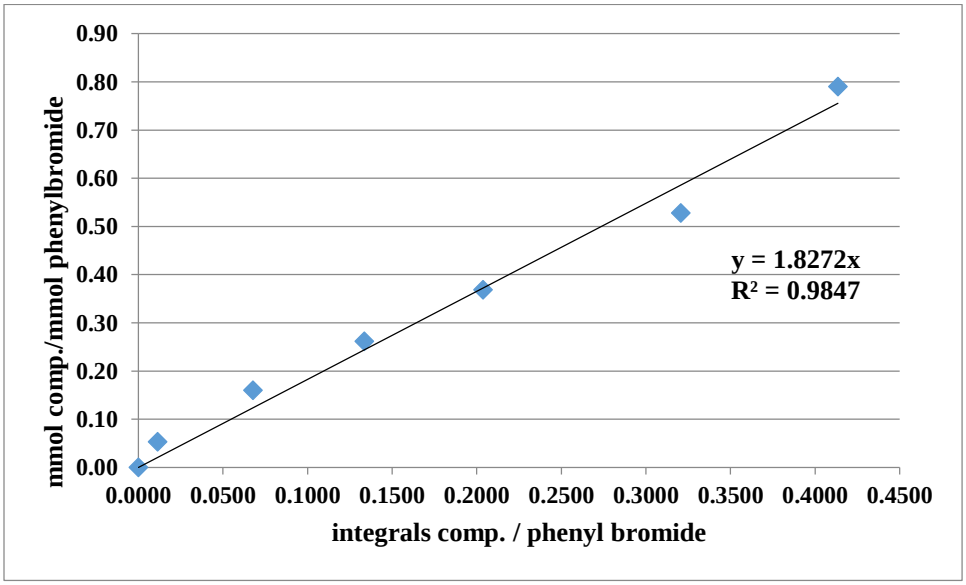

Figure 22: GC calibration curve for BTP.

5.2.3 Synthesis of Dicyanopyridine

Experiment can be found in 1VNA-52.

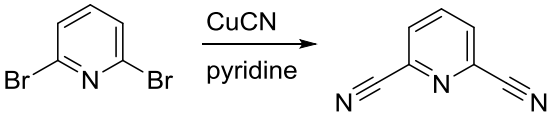

Scheme 13: Synthesis of dicyanopyridine.

Synthesis is based on a reaction by Baxter, et al., in 1992 (Scheme 13).[25] A large pressure vial was charged with 2.0 g (8 mmol) of dibromopyridine and 4 mL of pyridine. Before the copper

cyanide (CuCN) was added it was heated with a heat gun. This compound changed from a green to a brown color. This was done in order to remove the coordinated water. Afterwards, the CuCN was added (2.228 g, 24 mmol) along with another 4 mL of pyridine. This sealed vial was placed in a 150 °C oil bath behind a blast shield. This reacted for 24 hours and produced a thick black solution. This content was put into a separatory funnel along with 20 mL of concentrated KCN/H_2O to decomplex the copper from the pyridine. Dichloromethane (DCM) was added to the separatory funnel and mixed and the organic layer was removed and saved. This was done three times using 25 mL of DCM each time. The organic layer then separated using concentrated $NaCl/H_2O$ (Brine) three times, each using 25 ml. This was then evaporated to dryness producing a dark purple solid. To remove the color, activated charcoal was added and washed with DCM over a Büchner funnel to produce a clear, very light orange solution. This was also evaporated to dryness to produce a light beige product (1VNA-52). NMR of product was clean (Figure 23). ^1H NMR (500 MHz, $CDCl_3$): δ 8.08 ppm (t, J = 7.85 Hz, 1H), 7.93 ppm (d, J = 8.00 Hz, 2H).

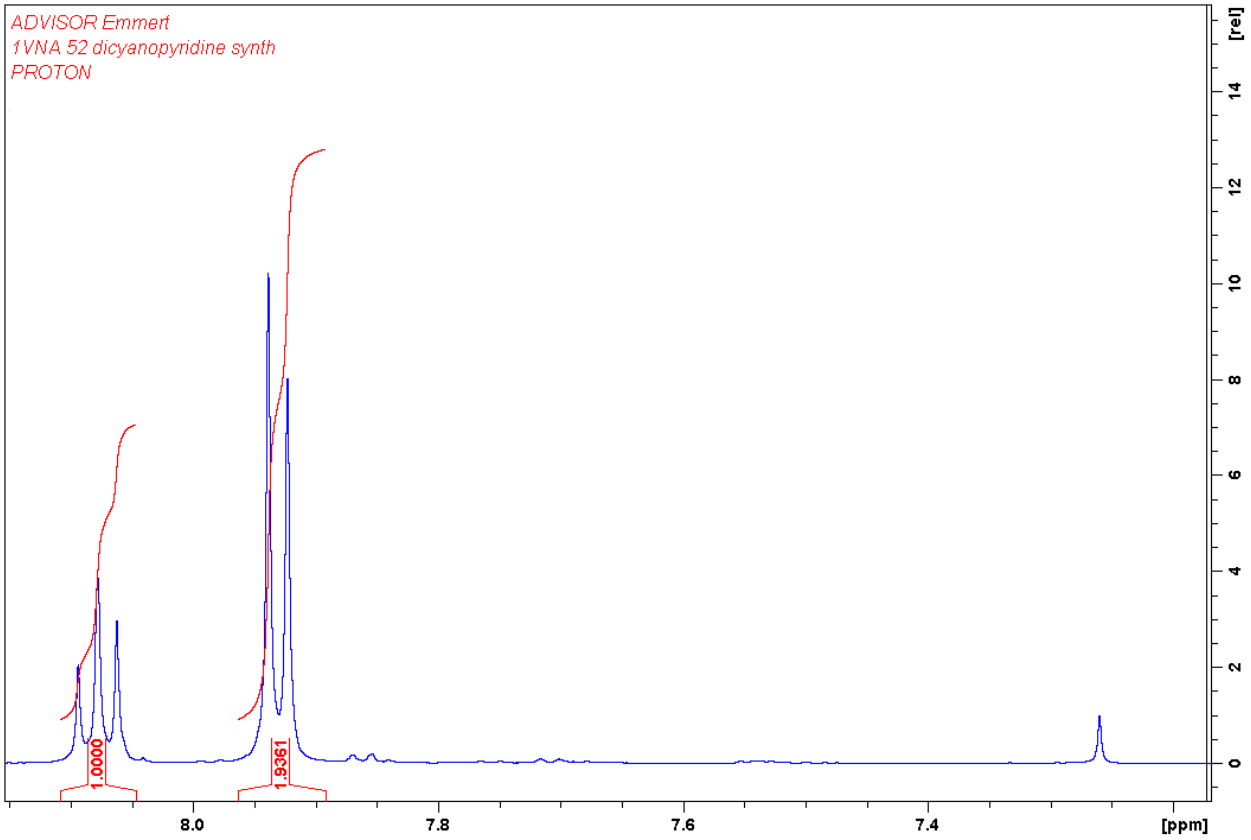

Figure 23: ^1H NMR of dicyanopyridine in $CDCl_3$.

5.2.4 Synthesis of Dicyanopyridine (Alternative)

Experiment can be found in 1VNA-5.

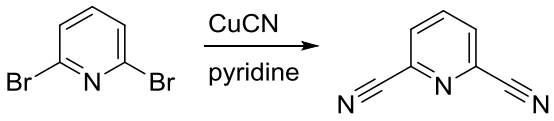

Scheme 14: Alternative synthesis of dicyanopyridine.

Synthesis is based on a reaction by Benson, et al., in 2014 (Scheme 14).[26] A 50 mL round bottom flask was charged with 2.5 g (10.5 mmol) of 2,6-dibromopyridine and dissolved in 20 mL of dimethylformamide (DMF). The resulting solution was yellow. The solution turned green when 1.5 g (16.5 mmol) of copper cyanide (CuCN) was added. Sodium cyanide (NaCN) was added (1.1 g, 22.5 mmol) and turned it into a thick brown solution. The flask was placed in an oil bat at 153 °C and refluxed overnight which produced a dark brown solution. The flask was allowed to cool to 25 °C before it was poured into 50 mL of UHP H_2O forming a brown precipitate. A dark yellow-brown solution formed when 10 mL of concentrated NaCN/H_2O was added to decomplex the copper from the pyridine. To isolate the product, extraction was conducted using a separatory funnel. Ethyl acetate was added, 25 ml, to being the extraction. The aqueous layer was extracted with 25 mL of chloroform three times. The entire organic layer was washed with 50 mL of UHP H_2O three times before it was evaporated to dryness. The resulting solid was mixed with 100 mL of UHP H_2O and collected over a Büchner funnel (1VNA-59). NMR was not very clean (Figure 24). ^{1}H NMR (500 MHz, $CDCl_3$): δ 8.06 ppm (t, J = 8.18 Hz, 1H), 7.91 ppm (d, J = 7.96 Hz, 2H).

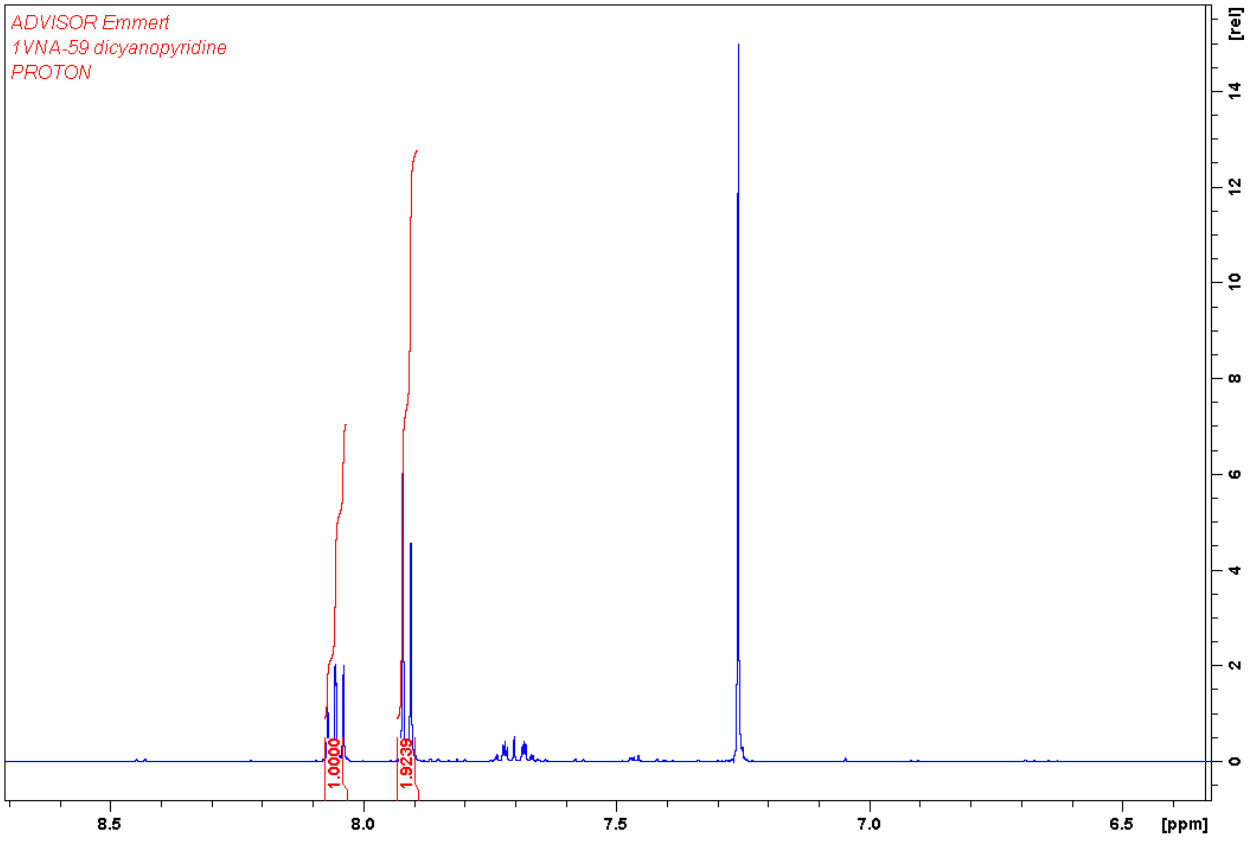

Figure 24: ^{1}H NMR of dicyanopyridine in $CDCl_3$.

5.2.5 Synthesis of Dicarbamidrazone Intermediate

Experiment can be found in 1HAF-19.

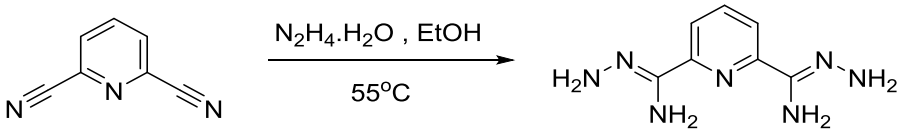

Scheme 15: Synthesis of dicarbamidrazone intermediate.

Synthesis is based on a reaction by Adam, et al., in 2013 (Scheme 15).[24] A 50 mL round bottom flask was flushed with nitrogen gas and charged with 1 g of dicyanopyridine (7.74 mmol, 1 eq.) and 15 ml of ethanol. Next, 3.75 ml of $N_2H_4.H_2O$ (77.4 mmol, 10 eq.) was added to the flask. Once the hydrazine monohydrate was added, the reaction turned an opaque yellow, and produced a pale yellow solid. The flask was placed in a hot oil bath at 55°C and stirred at 1500 RPM for five hours. The reaction was cooled to room temperature, and the product was washed

with water and diethyl ether through vacuum filtration. Product was left to dry overnight to provide a 93% yield (1HAF-19). Figure 25 shows the NMR of the product. ^{1}H NMR (500 MHz, DMSO-δ6): δ 7.81 ppm (*d*, *J* = 7.80 Hz, 2H), 7.64 ppm (*t*, *J* = 7.79 Hz, 1H), 6.03 ppm (*s*, 4H), 5.21 ppm (*s*, 4H).

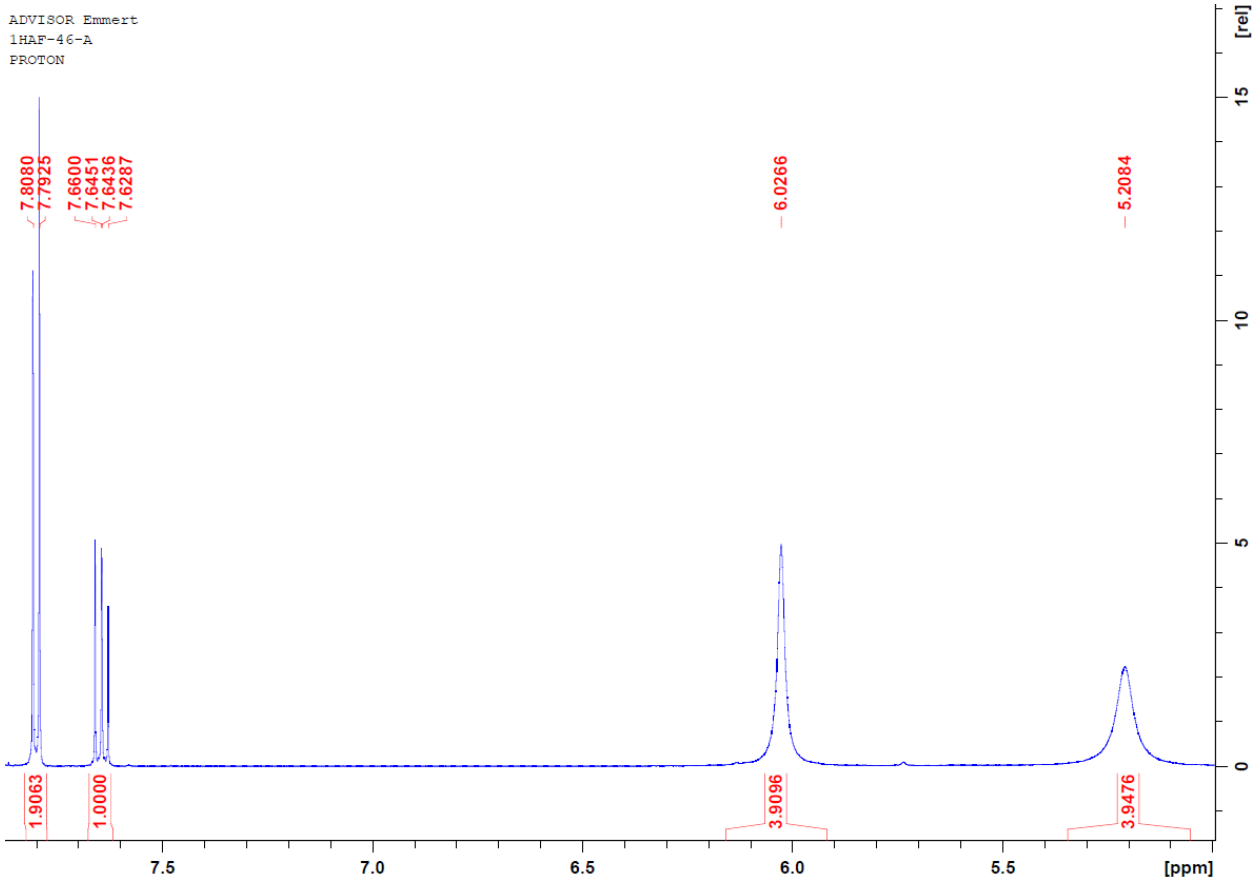

Figure 25: ^{1}H NMR of dicarbamidrazone intermediate in DMSO-δ6.

5.2.6 Synthesis of BTP from Dicarbamidrazone Intermediate

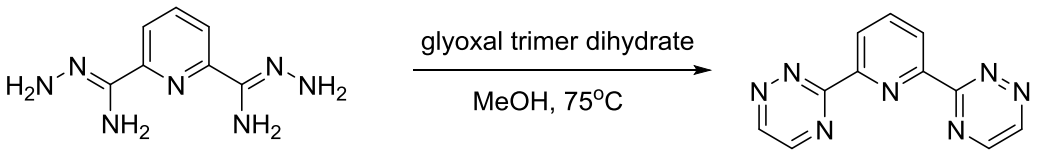

Scheme 16: Synthesis of BTP from dicarbamidrazone intermediate.

5.2.6.1. Synthesis from Literature

Experiment can be found in 1HAF-47.

At the start of the project, synthesis of BTP was based on a reaction by Kolarik, et al., in 1999(Scheme 16).[21] A 100 mL round bottom flask was charged with 0.67 g of dicarbamidrazone (3.472 mmol, 1 eq) and 30 mL of methanol. Added to the flask was 0.511 g of glyoxal trimer dihydrate (2.430 mmol, 0.7 eq) and the mixture was then stirred at 1500 rpm for two hours. The solution turned from an opaque white to a dark yellow. The mixture was then heated to 75°C in an oil bath for three hours, and turned from a dark yellow to a bright orange. After the reaction was complete, the solution was cooled to room temperature and washed with methanol *via* vacuum filtration. The reaction had an 82% yield (1HAF-47). However, the reaction was never clean, as shown by the impurities in the ^{1}H NMR (Figure 26). ^{1}H NMR (500 MHz, $CDCl_3$): δ 9.33 ppm (*d*, *J* = 2.35 Hz, 2H), 8.90 ppm (*d*, *J* = 2.39 Hz, 2H), 8.87 ppm (*d*, *J* = 7.87 Hz, 2H), 8.84 ppm (*d*, *J* = 2.41, impurity), 8.72 ppm (*d*, *J* = 1.12 Hz, impurity), 8.70 ppm (*d*, *J* = 1.03 Hz, impurity), 8.45 ppm (*s*, impurity), 8.21 ppm (*t*, J = 7.82 Hz, 1H), 8.06 ppm (*t*, 7.73 Hz, impurity).

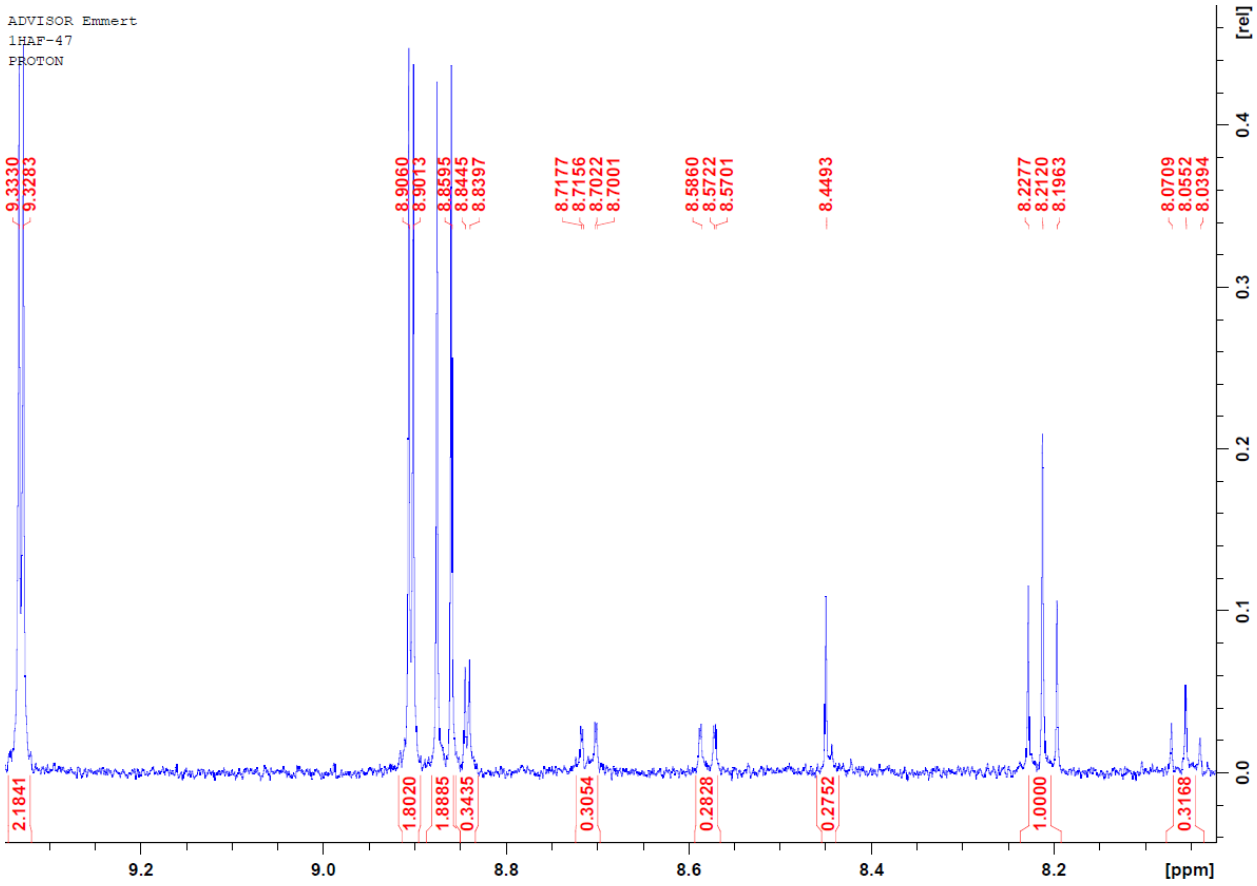

Figure 26: ^{1}H NMR of BTP in $CDCl_3$ showing impurities.

5.2.6.2 Purification of BTP

Experiments can be found in 1HAF-72 and 1HAF-81.

Several methods were tried to clean BTP. Recrystallization of BTP through layering was tried (1HAF-72). 0.1045 g of impure BTP was mixed with 15 ml of $CHCl_3$ and 2 ml of MeOH. Solution was heated until boiling. 20 ml of hot MeOH was layered on top. Solution was cooled to room temperature and then placed in the freezer over 48 hours.

A silica pad was used to purify BTP (1HAF-81). 0.0148 g of impure BTP was dissolved in a small amount of 5% MeOH in DCM. A silica pad with height 3.3 cm was packed and washed with DCM. A vacuum was used to pull the solvent through. BTP in solution was layered evenly on top of the silica. In fraction 1, more than 250 ml of DCM was sent through the silica pad. A clear solution came through and a spot of the fraction on a TLC plate under UV showed that there was no product in the fraction. In fraction 2, 100 ml of 2% MeOH and DCM was layered on top

and pulled through. Then, 100 ml of 3% MeOH in DCM was layered on top and pulled through. A clear solution came through that showed no product under UV light. In fraction 3, 100 ml of 5% MeOH in DCM was layered on top and pulled through. A light yellow solution came through. In fraction 4, 200 ml of 5% MeOH in DCM was layered on top and pulled through, giving a bright yellow solution. Fractions 3 and 4 were concentrated down through rotary evaporation and dried under vacuum overnight. The products were analyzed with ^{1}H NMR (Figure 27). ^{1}H NMR (500 MHz, $CDCl_3$): δ 9.33 ppm (*d*, *J* = 2.35 Hz, 2H), 8.90 ppm (*d*, *J* = 2.35 Hz, 2H), 8.86 ppm (*d*, *J* = 7.90 Hz, 2H), 8.21 ppm (*t*, *J* = 7.85 Hz, 1H).

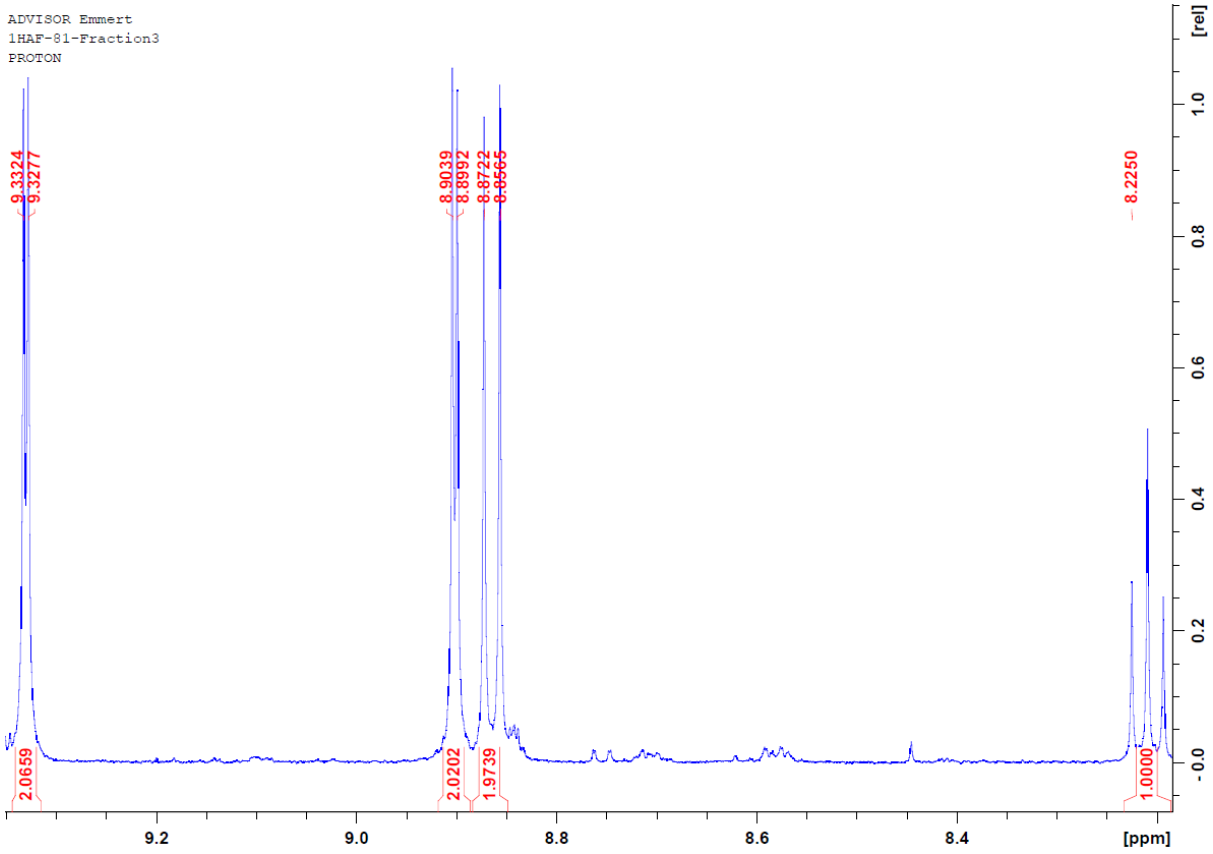

Figure 27: ^{1}H NMR of BTP purified with a silica pad in $CDCl_3$.

5.2.6.3. Optimization of Reaction

Experiments can be found in 1HAF-94.

The synthesis described in section 5.2.6.1 never produced clean product, and often had low yields. Work had to be done to optimize reaction conditions, and develop a reaction to produce

cleaner product (1HAF-94). The reaction was optimized by running nine different variations of the literature synthesis on a 0.010 g scale. Scheme 17 shows the variations done on the reactions. Reactions were done by charging 1 dram vials with glyoxal trimer dihydrate and 1 ml of MeOH which were stirred at 1500 RPM. 0.010 g of intermediate was added to the reaction mixture and the vial was flushed with N_2 gas and tightly capped. The vials were left to mix at room temperature and then heated to 75°C. When the reaction was complete, each of the vials were analyzed on the GC, as described in section 5.2.2.

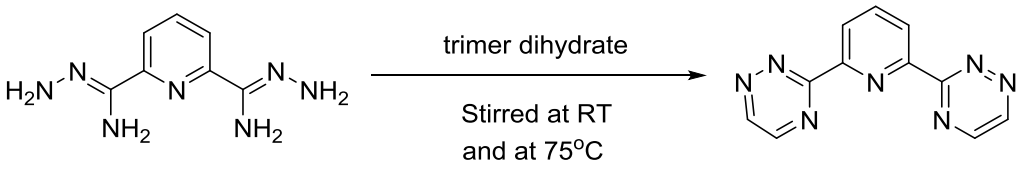

Sample	Equivalents of Glyoxal Trimer Dihydrate	Time stirring at RT (hr)	Time heating (hr)	Area % of Sample	Area % of PhBr	% Yield
1HAF-94-H	1	2	3	0.58	2.05	95
1HAF-94-C	1.4	3	2	0.55	2.41	77
1HAF-94-G	0.7	2	3	0.17	1.45	39
1HAF-94-E	1	2.5	o/n	0.19	1.85	34
1HAF-94-I	1.4	2	3	0.18	2.58	23
1HAF-94-B	1	3	2	0.091	1.75	17
1HAF-94-D	0.7	2.5	o/n	0.13	2.69	17
1HAF-94-F	1.4	2.5	o/n	0.054	1.87	10
1HAF-94-A	0.7	3	2	0.00046	1.69	0.09

Scheme 17: Optimization of BTP synthesis by changing reaction conditions.

5.2.6.4 Optimized BTP Synthesis

Experiment can be found in 1HAF-111.

By the end of the project, an optimized version of the literature synthesis of BTP, as described in section 5.2.6.1, was used. Work done in section 5.2.6.3 found the method that produced the most BTP. The solvent also proved to be very important to the reaction. Switching form MeOH to 99.8% analytically pure MeOH dried over activated sieves improved the purity of the BTP so that it was usable in extractions.

The new, optimized BTP synthesis followed the literature synthesis, but instead used 1 eq. of glyoxal trimer, 99.8% pure MeOH dried over molecular sieves, and the reaction was stirred at room temperature for 2 hours, and then heated to 75°C for 3 hours. This reaction resulted in a high percent yield of 95% (1HAF-111) and a much cleaner product, as confirmed by the NMR (Figure 28). ^{1}H NMR (500 MHz, $CDCl_3$): δ 9.33 ppm (*d*, *J* = 2.35 Hz, 2H), 8.90 ppm (*d*, *J* = 2.35 Hz, 2H), 8.86 ppm (*d*, *J* = 7.90 Hz, 2H), 8.21 ppm (*t*, *J* = 7.85 Hz, 1H).

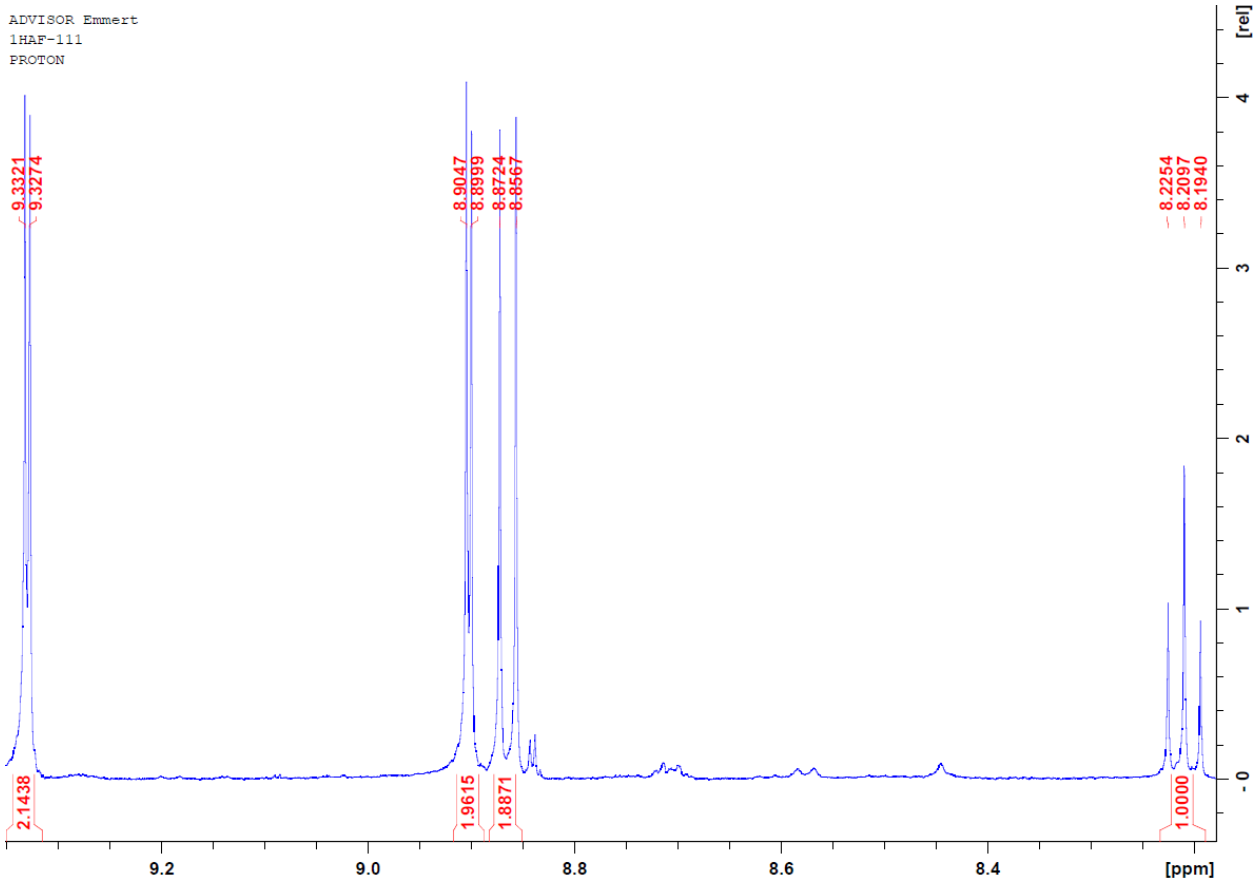

Figure 28: 1H NMR of optimized BTP synthesis using 99.8% MeOH dried over molecular sieves in $CDCl_3$.

5.2.6.5 BTP Recovered from Filtrate

Experiments can be found in 1HAF-89.

A small amount of BTP could be recovered from the filtrate of syntheses that produced impure BTP. The filtrate was concentrated down through rotary evaporation, and then left to dry under vacuum overnight. MeOH was added to the remaining residue, and sonicated for a few minutes. The mixture was filtered with vacuum filtration and left to dry overnight. The remaining solid was clean BTP, as confirmed by NMR (Figure 29). ^{1}H NMR (500 MHz, $CDCl_3$): δ 9.33 ppm (*d*, *J* = 2.45 Hz, 2H), 8.90 ppm (*d*, *J* = 2.37 Hz, 2H), 8.86 ppm (*d*, *J* = 7.94 Hz, 2H), 8.20 ppm (*t*, *J* = 8.01 Hz, 1H).

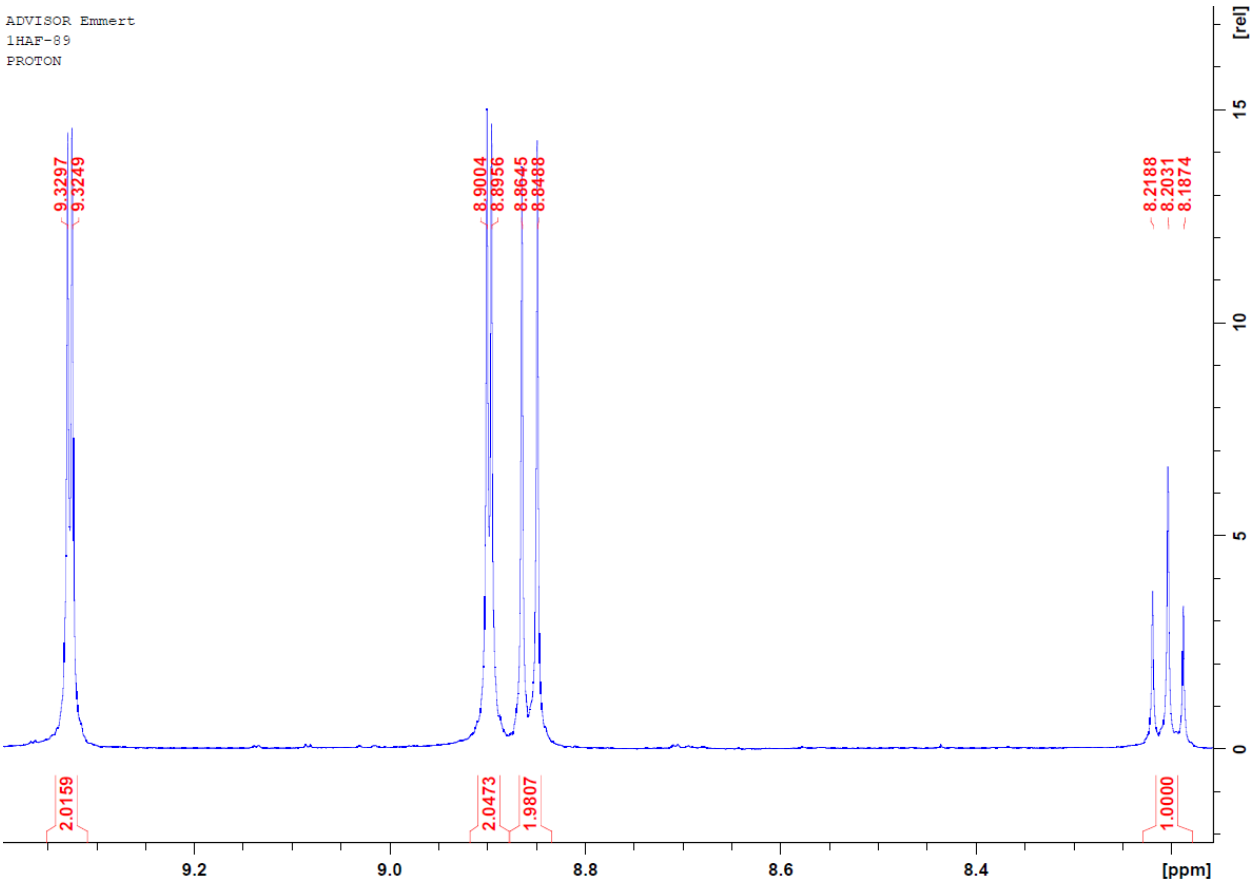

Figure 29: Clean 1H NMR of BTP recovered from filtrate in $CDCl_3$.

5.2.7 Synthesis of Me_4–BTP from Dicarbamidrazone Intermediate

Experiments can be found in 1VNA-20 and 1HAF-34.

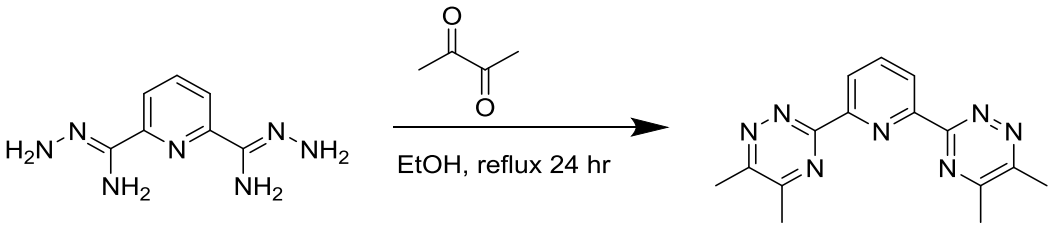

Scheme 18: Synthesis of Me_4-BTP.

Synthesis of Me_4-BTP was based on a reaction by Adam, et al., in 2013 (Scheme 18).[24] Me_4-BTP was synthesized from the same dicarbamidrazone intermediate as BTP. For reference to the reaction, see section 2.3.4. A 50 ml round bottom flask was flushed with nitrogen gas and charged with 1.00 g of the carbamidrazone intermediate (5.18 mm, 1 eq.), 20 ml of ethanol, and 1.135 ml of 2,3-butadione (12.94 mmol, 2.5 eq.). The flask was placed in a hot oil bath at 88°C and stirred at 1500 RPM under reflux for three hours. The reaction was cooled to room temperature and the reaction was dried through rotary evaporation. The solid was washed with ethyl acetate by vacuum filtration, and the product was left to dry overnight. Reaction had a 70% yield (1VNA-70). Most Me_4-BTP was clean enough to use in extractions immediately following (Figure 30). ^{1}H NMR (500 MHz, $CDCl_3$): δ 8.78 ppm (*d*, *J* = 7.86 Hz, 2H), 8.12 ppm (*t*, *J* = 7.85 Hz, 1H), 2.78 ppm (*s*, 6H), 2.71 ppm (*s*, 6H). Further purification could be done through recrystallization in a diffusion chamber. In a 1 dram vial, 10 mg of Me_4-BTP was dissolved in minimal amount of $CHCl_3$ and placed, uncapped, in a 20 dram vial containing EtOAc. The 20 dram vial was capped and placed in the freezer for three nights. Crystals formed were filtered and dried under vacuum.

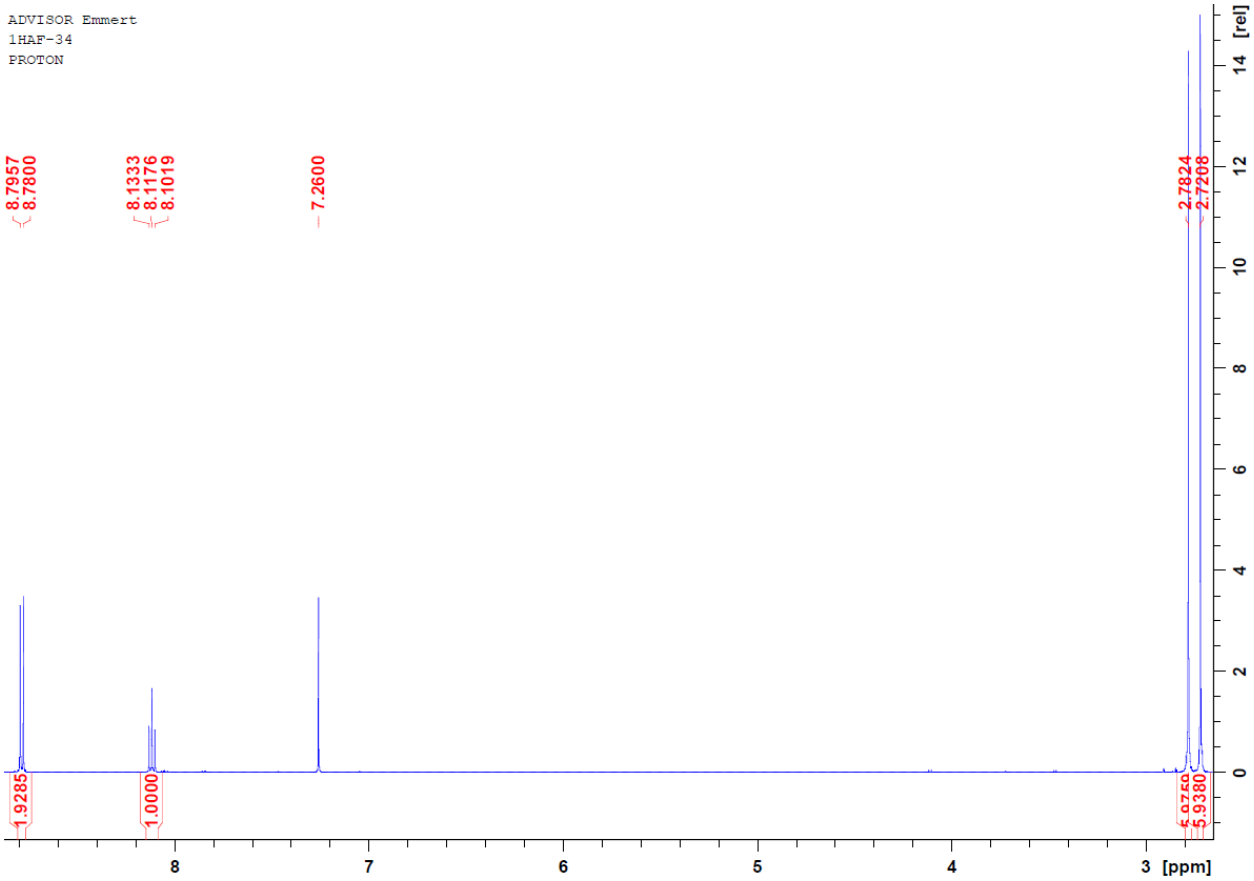

Figure 30: ^{1}H NMR of Me_4-BTP $CDCl_3$.

5.2.8 Synthesis: N-methoxy-N, 6-chloropyrizadine-2-carboxamide

Experiment can be found in 1VNA-63.

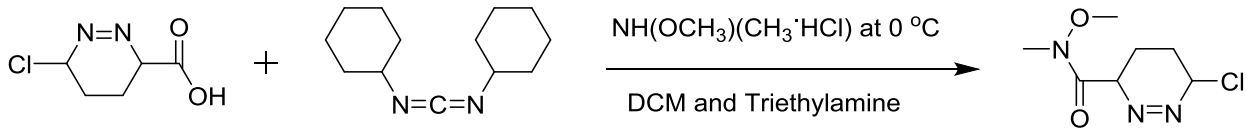

Scheme 19: Synthesis of N-methoxy-N, 6-chloropyrizadine-2-carboxamide.

Synthesis of N-methoxy-N, 6-chloropyrizadine-2-carboxamide was based on a reaction by Reddy et. al., in 2014 (Scheme 19).[27] A 100 mL round bottom was charged with 6-chloropyrizadine-2-carboyylic acid (1.0g, 6.31 mmol) and DCC (1.95 g, 9.46 mmol). The flask was put under nitrogen, chilled to 0 °C, 0.92 grams of $NH(OCH_3)(CH_3{\cdot}HCl)$ and stirred for 10 minutes. Triethylamine (1.32 mL, 9.46 mmol) and DCM (20 mL) was added to the reaction vessel

after it had reach room temperature and stirred for 24 hours (1VNA63). To purify the reaction and get the product, an extraction had to be run. The reaction vessel was diluted with UHP H_2O and extracted 2 times using 20 mL of ethyl acetate. The organic layer was washed with brine and dried over sodium sulfate. Large amounts of excess salts were first filtered out over a vaccum. Solvent was evaporated off using a rotovap producing a thick dark yellow-orange liquid. No solid form was obtainable, thus was a crude product, resulting in a yield of 1.316 grams or a 105% yield. This product was used in the next step immediately.

5.2.9 Synthesis of 1-(6-chloro-3,4,5,6-tetrahydropyridazin-3-yl)ethan-1-one

Experiment can be found in 1VNA-64.

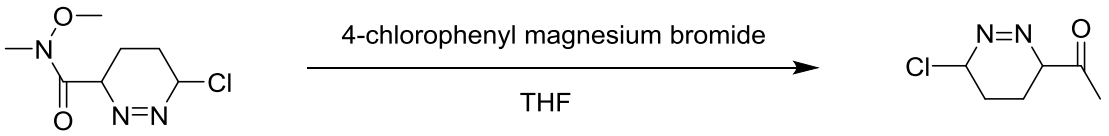

Scheme 20: Synthesis of 1-(6-chloro-3,4,5,6-tetrahydropyridazin-3-yl)ethan-1-one.

Synthesis of 1-(6-chloro-3,4,5,6-tetrahydropyridazin-3-yl)ethan-1-one was based on a reaction by Reddy et. al., in 2014 (Scheme 20).[27] A 50 mL round bottom was charged with N-methoxy-N, 6-chloropyrizadine-2-carboxamide (1.3164 g , 6.62 mmol), 10 mL of THF, and 4-chlorophenyl magnesium bromide (1.715 g, 0.794 mmol). These reagents were mixed under a nitrogen atmosphere at 0 ^oC for 5 minutes before the reaction was stirred at room temperature for 1 hour (1VNA-64). The reaction was quenched with saturated ammonium chloride and extracted twice with 20 mL of ethyl acetate. The organic layer was washed with brine and dried over sodium sulfate. Solvent was then evaporated off to produce a crude brown solid. This residue was then purified by column chromatography. Once the column was complete, TLC was run to determine which filtrate the product was in. The final compound was an off white solid (0.25 grams) resulting in a 24.5% yield (1VNA64).

5.3 Solubility Studies

5.3.1. BTP

Experiments can be found in 1VNA-19 and 1VNA-25.

It was important to develop a new solvent system that would better dissolve BTP or at least create a uniform suspension. Without a better solvent system, the amount of BTP that was actually put into each reaction vial caused large standard deviations. Since chloroform was not polar enough to uniformly dissolve the BTP, a more polar solvent was added to test the solubility. Table 2 shows 1 mL of total solvents and their respective ratios when trying to dissolve 13.6 mg of BTP in a 1 dram (1VNA-19).

Table 1: BTP solubility study solvent mixtures.

Sample	**Mixture**	**Ratio**
1VNA-19 A	Chloroform: Methanol	1 to 1
1VNA-19 B	Chloroform: Methanol	9 to 1
1VNA-19 C	Chloroform: Water	1 to 1
1VNA-19 D	Chloroform: Water	9 to 1
1VNA-19 E	Chloroform: Methanol: Water	2 to 1 to 1
1VNA-19 F	Chloroform: Methanol: Water	1 to 2 to 1
1VNA-19 G	Chloroform: Methanol: Water	1 to 1 to 2
1VNA-19 H	Chloroform: Methanol: Water	1 to 1 to 1

Each separate vial was shaken and photographed after ten minutes and then again at 72 hours as shown in Figure 31.

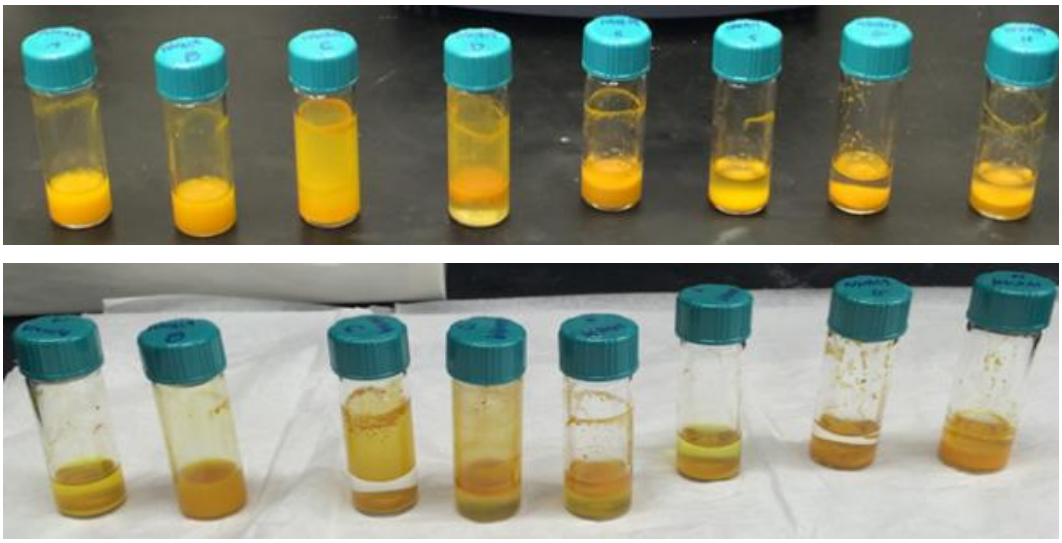

Figure 31: Solubility Study - Left to Right: 1:1 Chloroform: Methanol, 9:1 Chloroform: Methanol, 1:1 Chloroform: Water, 9:1 Chloroform: Water,2:1:1 Chloroform: Methanol: Water, 1:2:1 Chloroform: Methanol: Water, 1:1:2 Chloroform: Methanol: Water, 1:1:1 Chloroform: Methanol: Water. Top: 10 minutes Bottom 72 Hours.

Table 2 shows the mixtures and ratios used for chloroform and octanol, totaling 1 mL of solvents, and their respective ratios when trying to dissolve 13.6 mg of BTP in a 1 dram vial. These mixtures were all very similar in appearance after several hours. The vials were left to sit for a few days in order for a difference to become apparent (1VNA-25).

Table 2: BTP solubility: varying chloroform and octanol ratios.

Sample	**Mixture**	**Ratio**
1VNA-25 A	Chloroform: Octanol	9 to 1
1VNA-25 B	Chloroform: Octanol	5 to 1
1VNA-25 C	Chloroform: Octanol	8.5 to 1.5
1VNA-25 D	Chloroform: Octanol	19 to 1

5.3.2 Me_4-BTP

Experiments can be found in 1HAF-18 and 1HAF-21.

In order to determine the best solvent, 0.010 g of Me_4-BTP was added to 1 mL of solvent in a 1 dram vial. Solvents included $CHCl_3$, DCE, DCM, octan-1-ol, EtOAc, diethyl ether, PhCl, PhBr, $PhCF_3$, benzene, toluene, THF, MTBE, hexanes, and UHP H_2O.

5.4 Characterization of Ligands through ESI-MS

Experiments can be found in 1VNA-67 and 1HAF-109.

ESI-MS was used to characterize the ligand-REE complexes. ESI-MS were recorded using Thermo Finnigan LCQ deca spectrometer with a capillary voltage of 5 kV. A 5.9×10^{-4} M solution of BTP in MeOH was tested. A mixture of 5.9×10^{-4} M BTP and 2.2×10^{-5} M REE was tested.

In order to understand how BTP coordinates with an REE to extract it out of the aqueous phase, BTP and REE complexes were characterized through ESI-MS and ESI-MS/MS. As a solution of BTP and an REE was sent through the ESI when it is in the positive mode, the solution becomes ionized by H^+ and Na^+. A mass spectrometer attached to the ESI detected various complezes BTP formed with H^+, Na^+, the REE, itself, and any other ions in the solution. By analyzing the masses of the complexes shown on the spectra, we were able to infer the structure of the complex. For example, a peak on the spectra at 496.73 m/z could be a $NaBTP_2$ complex ($mass_{Na}$ = 22.99 g/mol, $mass_{BTP}$ = 237.23 g/mol, $mass_{NaBTP2}$ = 497.45 g/mol) Additionally, each REE analyzed had a unique isotopic splitting pattern, so any REE complex with BTP would show that same pattern.

Once a peak had been identified as a complex, it was confirmed with ESI-MS/MS. In this method, a peak was further ionized by increasing the ionization energy, and additional peaks would be formed as the molecule breaks apart. With ESI-MS/MS the structure of a complex can confirmed by observing ions and ligands break off from the molecule. Overall, this technique was used to predict ligand and REE complexes formed. To further support these predictions, ESI-MS/MS was used to further break apart and ionize the complexes. ESI-MS and ESI-MS/MS were used to characterize the REE and ligand complex, and as an additional prediction of whether the ligand would bind to an REE during an extraction.

5.5 Extraction Methods

Examples can be found in 1VNA-100 or 1HAF-100.

5.5.1. BTP Solution

A 10 ml volumetric flask was used to make a 0.05 M solution of BTP (0.136 g with a molar mass of 237 g/mol) in 19:1 $CHCl_3$: Octan-1-ol. BTP did not dissolve completely in this solvent system, but became a uniform suspension after sonicating in a water bath and vortexing. Solution had to be used quickly and shaken frequently to maintain uniform suspension and prevent separation of $CHCl_3$ and octan-1-ol. Not all BTP went into solution.

5.5.2. Me_4-BTP Solution

A 10 ml volumetric flask was used to make a 0.05 M solution of Me_4-BTP (0.147 g with a molar mass of 293.33 g/mol) in $CHCl_3$. Me_4-BTP dissolved completely in solvent.

5.5.3. Rare Earth Metal Solution

A 10 ml volumetric flask was used to make a 0.002 M solution of $REE(NO_3)_3.6H_2O$ in an acid solution. Rare earth metal, acid, and acid concentration varied depending on the experiment. Later experiments also included a salt in the solution at a 0.006 M concentration. Other experiments contained a mixture of REEs, all at a concentration of 0.002 M.

5.5.4. Extraction Procedure

Experiments can be found in 1HAF-1 and 1VNA-5.

A 500 μL glass syringe was used to add 0.5 ml of rare earth metal solution and 0.5 ml of either the BTP solution of Me_4-BTP solution to a one dram vial. Samples were made in triplicate and shaken at 800 RPM for 1, 2, and 4 hours at room temperature. Earlier experiments also included 3 and 24 hours. After being shaken, the aqueous phase was removed from the organic phase using a sterile glass pipette. In some cases, the samples had to be left still for the phases to separate. The sample was then prepared for the ICP-OES by diluting 100 μL of the aqueous phase

to 10 mL with Ultra High Purity (UHP) water. For a 0 hour data point, 100 μL of the rare earth metal standard solution was also diluted to 10 ml.

5.5.5 Inductively Coupled Plasma Optical Emission Spectrometer (ICP-OES)

ICP-PES was used to measure the concentration of rare earth metal in solution. ICP-OES measurements were performed on a Perkin Elmer Optima^{TM} 8000, and calibrated using UHP H_2O, and solutions of 0.1, 1, and 10 ppm made from a 10 ppm stock multi-element standard obtained from Perkin-Elmer.

Equation 2 was used to determine the percent extraction of rare earth metal into the organic phase for a length of time each phase was allowed to react:

$$\frac{Avg([REE]_0) - Avg([REE]_x)}{Avg([REE]_0)} \times 100\% = \%Extraction\ at\ x\ hours$$

Equation 3

In the equation, Avg($[REE]_0$) is the average REE concentration of the three samples shaken at 0 hours and Avg($[REE]_x$) is the average REE concentration of the three samples shaken at x hours.

The distribution ratio of an REE, or the measure of how well the metal is extracted, is determined by Equation 3.

$$D_A = [M_A]_{org}/[M_A]_{aq}$$

Equation 4

The selectivity fraction of two REEs, which compares how well one REE is extracted over another, is determined by Equation 4.

$$SF = D_A/D_B$$

Equation 5

5.6 Acid Optimization Studies

Experiments can be found in 1HAF-28, 1HAF-49, 1HAF-53, 1VNA-26, and 1VNA-27

5.6.1 Best Acid

Different acids were tested to find which yielded the highest percent extraction. Acids used included HCl, HNO_3, and H_2SO_4.

5.6.2 Best Concentration

Different concentrations were tested to find which yielded the highest percent extraction. Concentrations used included 0.001 M, 0.01 M, and 0.1 M. Thus far, the 0.001 M concentration has produced the highest extraction percentages.

5.7 Salt Optimization Studies

Experiments can be found in 1VNA-40 through 1VNA-49.

Different salts were tested to find which yielded the highest percent extraction. Salts used included were NaCl, NaBr, $NaNO_3$, $NaNO_2$, KNO_3, and KOAc. These salts were added individually at a concentration of 0.006 M to the optimized extraction protocol described in section 5.5.4. The addition of potassium salts has helped produced the highest extraction percentages so far. The slightly larger ionic radius may coordinate to the rare earth and ligand complex more effectively.

References

1. Hughes, I. D.; Dane, M.; Ernst, A.; Hergert, W.; Luders, M.; Poulter, J.; Staunton, J. B.; Svane, A.; Szotek, Z.; Temmerman, W. M., Lanthanide contraction and magnetism in the heavy rare earth elements. *Nature* **2007,** *446* (7136), 650-653.

2. Goldschmidt, V. M.; Barth, T. F. W., *Geochemische Verteilungsgesetze der Elemente 5. 5*. Ja. Dybwad: Oslo, Kristiania, 1925.

3. Weeks, M. E., The discovery of the elements. XVI. The rare earth elements. *Journal of Chemical Education* **1932,** *9* (10), 1751.

4. A National Historic Chemical Landmark: Separation of Rare Earth Elements. American Chemical Society: Durham, NH, 1999.

5. Rare Earth Elements: A Review of Production, Processing, Recycling, and Associated Environmental Issues. U.S. Environmental Protection Agency: Cincinnati, OH, 2012.

6. Gambogi, J., Rare Earths. Survey, U. S. G., Ed. 2016.

7. *Minerals, Critical Minerals, and the U.S. Economy*; National Research Council of the National Academies: Washington, DC, 2007.

8. Talens Peiró, L.; Villalba Méndez, G., Material and Energy Requirement for Rare Earth Production. *JOM* **2013,** *65* (10), 1327-1340.

9. Molycorp, Molycorp Announces Start-up of Heavy Rare Earth Concentrate Operations at Mountain Pass, Calif. 2012.

10. Miller, J. W.; Zheng, A., Molycorp Files for Bankruptcy. *The Wall Street Journal* **2015**.

11. Mineral Commodity Summaries, January 2015. U.S. Geological Survey: 2014.

12. Rare Earth Elements - Critical Resources for High Technology. U.S. Geological Survey: 2002.

13. Mineral Commodity Summaries 2007. U.S. Geological Survey: Washington DC.

14. Anand, T.; Mishra, B.; Apelian, D.; Blanpain, B., TMS Partners in Progress: The case for recycling of rare earth metals—A CR3 communication. *JOM* **2011,** *63* (6), 8-9.

15. *Mineral commodity summaries 2015*; Reston, VA.

16. Du, X.; Graedel, T. E., Global In-Use Stocks of the Rare Earth Elements: A First Estimate. *Environmental Science & Technology* **2011,** *45* (9), 4096-4101.

17. Hirano, S.; Suzuki, K. T., Exposure, metabolism, and toxicity of rare earths and related compounds. *Environmental Health Perspectives* **1996,** *104* (Suppl 1), 85-95.

18. Bandara, H. M. D.; Field, K. D.; Emmert, M. H., Rare earth recovery from end-of-life motors employing green chemistry design principles. *Green Chemistry* **2016,** *18* (3), 753-759.

19. Inoue, K.; Alam, S., Refining and Mutual Separation of Rare Earths Using Biomass Wastes. *JOM* **2013,** *65* (10), 1341-1347.

20. Quinn, J. E.; Soldenhoff, K. H.; Stevens, G. W.; Lengkeek, N. A., Solvent extraction of rare earth elements using phosphonic/phosphinic acid mixtures. *Hydrometallurgy* **2015,** *157*, 298-305.

21. Kolarik, Z.; Müllich, U.; Gassner, F., SELECTIVE EXTRACTION OF Am(III) OVER Eu(III) BY 2,6-DITRIAZOLYL- AND 2,6-DITRIAZINYLPYRIDINES. *Solvent Extraction and Ion Exchange* **1999,** *17* (1), 23-32.

22. Geist, A.; Hill, C.; Modolo, G.; Foreman, M. R. S. J.; Weigl, M.; Gompper, K.; Hudson, M. J., 6,6′-Bis(5,5,8,8-tetramethyl-5,6,7,8-tetrahydro-benzo[1,2,4]triazin-3-yl) [2,2′]bipyridine, an Effective Extracting Agent for the Separation of Americium(III) and Curium(III) from the Lanthanides. *Solvent Extraction and Ion Exchange* **2006,** *24* (4), 463-483.

23. Guassian 09 User's Reference. http://www.gaussian.com/g_tech/g_ur/k_freq.htm (accessed March 21 2016).

24. Adam, C.; Kaden, P.; Beele, B. B.; Mullich, U.; Trumm, S.; Geist, A.; Panak, P. J.; Denecke, M. A., Evidence for covalence in a N-donor complex of americium(iii). *Dalton Transactions* **2013,** *42* (39), 14068-14074.

25. Baxter, P. N. W.; Connor, J. A.; Schweizer, W. B.; Wallis, J. D., Novel tetra- and hexa-dentate ligands from 6,6[prime or minute]-dicyano-2,2[prime or minute]-bipyridine. *Journal of the Chemical Society, Dalton Transactions* **1992,** (20), 3015-3019.

26. Benson, C. R.; Hui, A. K.; Parimal, K.; Cook, B. J.; Chen, C.-H.; Lord, R. L.; Flood, A. H.; Caulton, K. G., Multiplying the electron storage capacity of a bis-tetrazine pincer ligand. *Dalton Transactions* **2014,** *43* (17), 6513-6524.

27. Reddy, S. M.; Reddy, S. M.; Reddy, B. N.; Pathak, M., Synthesis and antimicrobial activity studies of microwave irradiated in (4-chlorophenyl) (6-methylpyridin-3-yl) derivatives. *Der pharma chemica* **2014,** *6* (6), 435-441.